Computers & Operations Research 185 (2026) 107293

Contents lists available at ScienceDirect

Computers and Operations Research

journal homepage: www.elsevier.com/locate/cor

Optimizing production–transportation–delivery in global supply chain with demand ambiguity by branch-and-cut algorithm

Zheng Wang [a,b], Pingyuan Dong [a], Ying Liu [c,*]

[a] College of Mathematics and Information Science, Hebei University, Baoding 071002, China
[b] Nanyang Tobacco Company Oilfield Branch, Nanyang 47300, China
[c] Key Laboratory of Machine Learning & Computational Intelligence, College of Mathematics and Information Science, Hebei University, Baoding 071002, China

ARTICLE INFO

Keywords:
Global supply chain
Horizontal cooperation
Demand ambiguity
Globalized distributionally robust optimization
Branch-and-Cut

ABSTRACT

The complexity incorporated in global supply chain (GSC) means the production, transportation, and delivery are totally operating and completing in the dynamic business environment with unforeseen events. At present, there are two key challenges in the transnational supply chain network: addressing the demand ambiguity and enhancing cooperation among supply chain entities. To optimize the production–transportation–delivery decision in GSC, a novel globalized distributionally robust GSC (GDR-GSC) model with horizontal cooperation is proposed, in which the ambiguity of demand distribution is characterized by inner and outer ambiguity sets. Subsequently, the proposed model is transformed into mixed integer nonlinear programming (MINLP) model by duality theory. It is commonly difficult to solve in high-dimensional case. Therefore, a customized Branch-and-Cut (B&C) algorithm tailored for the GDR-GSC model is designed to handle complex MINLP problems, and improves computational efficiency and solution quality. The case study based on Apple's sales operations in China and Malaysia demonstrates the effectiveness and superiority of the B&C algorithm in solving the GDR-GSC model. Numerical experiments show that the customized B&C algorithm can improve the average solving time by 18% while maintaining the same solution quality. Based on realistic cases, we know that horizontal cooperation can increase profits by at least 6.25%.

1. Introduction

Global supply chain (GSC) refers to the worldwide network of businesses, organizations, and activities involved in the production and distribution of goods and services from raw materials to end consumers. This network includes suppliers, manufacturers, transportation providers, distributors, retailers, and customers, all interconnected through complex logistical, financial, and informational processes. The goal of the GSC is to efficiently manage the flow of products and services across international borders to meet consumer demand and optimize business operations (Khan, 2020). Nowadays, multinational corporations face mounting challenges in managing their GSCs, since production, transportation, and delivery activities span multiple countries. Hereinto, there are mainly two difficulties in the GSC need to be solved: (1) How to accurately depict the customer demand? (2) How to strengthen cooperation among some links in the supply chain to reduce costs?

Due to market fluctuations and policy impacts, customer demand is often uncertain. The uncertain parameter in the model significantly increases the complexity of optimization, as the uncertainty may affect the feasibility and stability of the solution (Hasani et al., 2021; Wang et al., 2025). To address this issue, two major frameworks are typically used: stochastic optimization (SO) and robust optimization (RO). SO assumes that uncertain parameter follows a known probability distribution, and solves the problem by optimizing the expected value or by meeting the objective function at a certain confidence level (Birge and Louveaux, 2011). This method is suitable for scenarios where the distribution of uncertainty can be estimated with reasonable accuracy. However, in practical applications, it is often difficult to obtain precise probabilistic information of customer demand, limiting the applicability of SO in complex uncertain environments. RO assumes that uncertain parameter varies within a known set and addresses uncertainty by optimizing the worst-case outcome. RO focuses more on feasibility, ensuring that the solution remains feasible regardless of how the distribution of uncertain parameters changes (Ben-Tal et al., 2009). Therefore, traditional RO can sometimes lead to overly conservative solutions, which may limit the potential for maximizing returns. Therefore, to a certain extent, these traditional optimization methods

* Corresponding author.
E-mail address: yingliu@hbu.edu.cn (Y. Liu).

https://doi.org/10.1016/j.cor.2025.107293
Received 21 November 2024; Received in revised form 6 August 2025; Accepted 27 September 2025
Available online 3 October 2025

tend to be overly conservative or inefficient, necessitating more flexible and robust optimization approaches to handle such problems.

Distributionally robust optimization (DRO) seeks the worst-case optimality under given partial distribution information about the parameters (Saif and Madani, 2022; Wang et al., 2024b). The core idea of this method in handling uncertainty is to strictly limit constraints within the ambiguity set of distributions to meet feasibility requirements. However, in GSC problems, due to the cross-border heterogeneity and dynamic complexity of customer demand, the situation that the true distribution of parameters is excluded from the ambiguity set is particularly prominent. Specifically, first, demand data in transnational supply chains are often scattered across different regions, resulting in limited historical samples and insufficient representativeness (Timmer et al., 2021). Second, cross-border disruptive events such as geopolitical conflicts and global pandemics occur frequently, and the demand impact of such low-probability events often exceeds the modeling boundaries of traditional ambiguity sets (Yang, 2021). In fact, the escape of the true distribution from the ambiguity set is a frequent and critical challenge in GSCs. The statistics show that 70% of multinational enterprises experience at least one disruption caused by this phenomenon each year, resulting in significant losses (World Economic Forum, 2022). Unlike traditional DRO which lacks escape-response mechanisms, the globalized distributionally robust optimization (GDRO) (Liu et al., 2023) employs two ambiguity sets: the inner set enforces operational stability in high-probability scenarios, while the outer set enables controlled adjustments during distribution escapes—ensuring both baseline robustness and adaptive resilience in complex environments.

Horizontal cooperation is an effective strategy to improve operational efficiency and responsiveness, especially in the face of fluctuations and uncertainties in global market demand. Horizontal cooperation in the GSC refers to collaboration between companies at the same stage of the supply chain, typically competitors or peers, working together to share resources, reduce costs, and improve efficiency (Hosseinnezhad et al., 2023). For example, warehouses in different regions can coordinate and share inventory, thereby reducing logistics costs and improving the resilience of the supply chain (Li et al., 2012; Yang et al., 2017; Wu and Shang, 2021). The uncertainty factors and considered horizontal cooperation make the GSC model more complex, and solving it will be a huge challenge. The current commercial solvers have taken shape for solving complex problems, but some specific types of problems still take a long time to explore feasible solutions. At this time, it is necessary to design heuristic algorithms or exact algorithms for specific problems (Tsai and Chao, 2009; Enayati and Özaltın, 2024). Therefore, how to effectively solve our GSC production, transportation and delivery problems remains a challenge.

Driven by the reasons mentioned above, this paper presents a novel globalized distributionally robust global supply chain (GDR-GSC) model to optimize the production, transportation, and delivery processes in a multinational supply chain under demand ambiguity. The core of this model is the GDRO framework simultaneously incorporates distributional uncertainty and model errors, delivering critical advantages for global supply chain challenges. The GDRO approach addresses dual complexity through integrated risk control: it avoids deterministic overreliance while mitigating extreme-scenario risks, and resolves the inherent trade-off between core-scenario stability and extreme-scenario adaptability (Shi et al., 2013; Duan et al., 2023). The single ambiguity sets or rigid constraints often lead to risk operational rigidity when over-constrained, or reliability loss happens when under-constrained. Differently, GDR-GSC model employs a hierarchical ambiguity structure. The inner set (core constraint region) enforces strict satisfaction of robust constraints for high-probability demand scenarios, ensuring stable core-market supply; The outer set covers low-probability extreme events (e.g., regional demand surges), permitting tolerable constraint violations within model-error margins to balance risk containment and operational flexibility (Liu et al., 2023). This framework enables enterprises to maximize efficiency and profitability while minimizing risks in uncertain environments.

Another key aspect of the model is the exploration of horizontal cooperation among warehouses at the same level within multinational corporations. By sharing customer location and demand historical data, warehouses can significantly streamline distribution processes and lower delivery costs. This cooperation enhances responsiveness to demand fluctuations and improves resource allocation across the supply chain. However, implementing such cooperation is complex. For multiple warehouses to function cohesively, the distribution network evolves into a vehicle routing problem (VRP), a well-known NP-hard challenge. As the number of customers and warehouses grows, the problem's complexity increases exponentially, making traditional methods inadequate for quickly finding optimal solutions. To address this issue, we employ the B&C algorithm, an exact method that dynamically adds new constraints during the solution process, effectively narrowing the search space. To enhance efficiency further, we introduce a special ordered set (SOS) branching combined pseudo shadow price (PSP) branching and a customized k-path cut. The k-path cut is a specific cutting plane approach that accelerates the search for optimal solution in these complex scenarios. Through numerical experiments, we conclude that the customized B&C algorithm can significantly improve computational speed while maintaining the optimal solution. Subsequently, we validate the feasibility of the model using real-world cases, and the results demonstrate that the horizontal cooperation strategy effectively reduces supply chain costs. Additionally, we analyze the role of key parameters and thoroughly explore the impact of these parameter changes on the model's outcomes, revealing potential insights for management decision-making.

Based on the prementioned statements, the GDR-GSC model not only significantly reduces delivery costs but also effectively manages customer demand fluctuations in complex supply chain networks. The horizontal cooperation strengthens multinational corporations' competitiveness in GSC management. Here are the main contributions of this paper:

- We introduce a GDR-GSC model that effectively tackles the issue of demand ambiguity commonly faced in GSCs. By incorporating GDRO method, the inner and outer ambiguity sets are utilized, which allows us to comprehensively manage worst-case scenarios and demand uncertainties. This ensures robust decision-making capabilities that can withstand variable market conditions.
- Our GDR-GSC model further integrates horizontal cooperation strategies among warehouses, which is an effectual approach to GSC management. By facilitating the sharing of customer information and coordinating vehicle routing among different warehouses, our model not only increases supply chain flexibility but also reduces operational costs and mitigates potential risks. This tactic offers a more resilient and efficient solution to the various challenges faced in GSCs, ultimately contributing to better overall performance.
- A customized B&C algorithm is developed specifically for our GDR-GSC model, which significantly enhances both computational efficiency and solution quality by incorporating joint branching strategy and strengthened k-path cuts. This tailored algorithm optimizes key decisions related to production, transportation, and delivery across multinational supply chain networks, enabling faster and more accurate solutions.

The structure of the upcoming sections is as follows: Section 2 presents the literature review. In Section 3, we formulate the model, followed by a detailed analysis in Section 4. Section 5 introduces a customized B&C algorithm for the GDR-GSC model and evaluates the performance of the algorithm. In Section 6, we apply the model to a real-world case study and analyze the effects of different parameters, comparing the situations with and without of horizontal cooperation and the differences among different models. Finally, Section 8 summarizes our conclusions.

2. Literature review

In this section, we review our paper in three parts to better explore research gap and state our study.

2.1. Global supply chain with cooperation

GSC management is a critical area of focus, with recent research emphasizing multiple aspects (Zhen et al., 2019; Tokito et al., 2023). Hasani et al. (2021) developed a robust multi-objective optimization model that configured a green GSC network, considering disruptions and focusing on economic and environmental aspects. Sarkar et al. (2022) aimed to nullify food waste in a two-stage parallel supply chain.

General GSCs often lack efficiency. The integration of cooperation within GSC strategies has garnered significant attention due to its potential to enhance operational synergies and bolster market presence. Li et al. (2022) explored the application of carbon emissions trading policies in supply chain management and how to achieve overall emission reduction goals through reasonable cooperation models. Wang et al. (2024c) aimed to provide a clearer understanding of the cooperation patterns and their impact on the supply chain during the COVID-19 pandemic. However, in recent years, there has been little research on horizontal cooperation on the same tier in the GSC. Horizontal cooperation is a multifaceted approach that holds promise for advancing supply chain objectives across economic, environmental, and social dimensions. It offers a pathway for supply chain actors to navigate the intricacies of a global marketplace, where cooperation can lead to mutual gains and collective resilience.

2.2. Uncertainty in global supply chain

Uncertainty in the GSC has emerged as a significant challenge, stemming from various sources such as demand fluctuations (Sirikasemsuk and Luong, 2017), supply instabilities (Nguyen and Chen, 2018), and production delays (Niu et al., 2023). To address these uncertainties, researchers have proposed a range of strategies and models aimed at enhancing the resilience and agility of supply chains. Lalmazloumian et al. (2016) used a RO approach to handle uncertainties in procurement, production, and distribution costs. Kim et al. (2018) developed a mixed-integer optimization model along with robust counterparts to address the uncertainties of recycled products and customer demand in the fashion industry. Chen et al. (2024) presented a multi-product, multi-period construction supply chain model that accounted for supplier capacity and material demand uncertainties, using RO to address these uncertainties. When dealing with different uncertain parameters, different approaches are taken. In cases when partial distribution information of uncertain parameters is known, previous research often employs DRO method (Qu et al., 2017; Wang et al., 2024a; Wei et al., 2024). Petridis et al. (2023) tackled uncertainty risk in supply chain design by adopting SO approach. Zhang et al. (2022) established a bi-objective DRO model to balance transportation time and safety, considering demand, transportation time, freight costs, and safety coefficients as uncertain variables with partial distribution information. Gao et al. (2024) utilized DRO approach to address uncertainties in purchasing cost, carbon emissions, and demand problem. Recently, Liu et al. (2023) proposed the GDRO method, which is more suitable for our complex GSC problem with distributional ambiguity of demand. Compared to previous methods, GDRO method effectively reduces the conservativeness of the model when dealing with uncertainty, thereby avoiding profit loss or cost increases caused by excessive conservativeness. At the same time, this method does not significantly increase computational complexity, making it highly efficient for large-scale optimization problems. Therefore, in this paper, we take this approach to optimize production, transportation and delivery in the GSC.

2.3. Method of solution

In GSC problems, large-scale integer programming models are often involved, which are difficult to solve directly using commercial solvers. Many scholars employed customized heuristic or exact algorithms to increase solution efficiency (Koyuncuoğlu and Demir, 2023; Bakhshi Sasi et al., 2024). A multicut version of the Benders decomposition approach for handling two-stage stochastic linear programming challenges was introduced by You and Grossmann (2013). Computational studies demonstrated that this approach provided significant CPU time savings compared to the standard method while effectively dealing with large-scale problems. Peivastehgar et al. (2023) minimized greenhouse gas emissions and costs in a bi-objective production routing problem using a hybrid of branch-and-bound and multi-objective fuzzy goal programming. Elyasi et al. (2024) emphasized the importance of flexible manufacturing systems in addressing demand ambiguity and provided an effective solution through a column generation-based heuristic algorithm. Not all heuristic or exact algorithms can accelerate problem-solving; only those specifically tailored to particular problems can significantly enhance solution efficiency. This is because different problems possess unique structures and characteristics, and general algorithms may fail to effectively leverage these features for optimization. By thoroughly analyzing the problem's attributes and designing targeted algorithms in this paper, it is possible to better capture the complexity within the problem, reduce unnecessary computations, and thereby improve the speed of finding solutions.

2.4. Research gap and our study

Table 1 shows some relevant works and makes a comparison between our study and them in line with critical factors so as to offer a general perspective. From Table 1, we find the following research gaps:

- In the study of GSCs, cooperative strategies have been substantial implemented. Studies such as Soysal et al. (2018), Fan et al. (2020), and Hacardiaux and Tancrez (2022) have examined the impact of horizontal cooperation on supply chains, while (Saeed, 2013) has focused on the effects of vertical cooperation strategies. Especially, Yazdekhasti et al. (2021) has explored both forms of cooperation, and regarded that horizontal cooperation has more advantages than vertical cooperation. It is notable that, the cooperation strategies studied by these scholars are commonly the cooperations among different companies within the supply chain. The adoption of such cooperation strategies will result in the problem of unbalanced benefit distribution. There is little research that considers the cooperation of different distributors of the same multinational. Nevertheless, it can maximize the benefits of the multinational corporation and reduce costs throughout the supply chain.
- Many researchers have also considered uncertainties within supply chains, in which some addressed cost uncertainties (Petridis et al., 2023; Zhao et al., 2024). But most of them focused on demand uncertainties, as seen in You and Grossmann (2013), Dong and Yuan (2025), Elyasi et al. (2024), and Chen et al. (2024). Moreover, in the literature that captured the uncertainty of demand, few studies considered complex ambiguity of demand distribution, and characterized it with inner and outer ambiguous distribution sets.
- To address these uncertainties, methods including those proposed in You and Grossmann (2013), Yazdekhasti et al. (2021), Petridis et al. (2023), Elyasi et al. (2024) for SO, Kim et al. (2018), Hasani et al. (2021), Chen et al. (2024) for RO, and Dong and Yuan (2025), Zhao et al. (2024) for DRO have been considered. Most optimization methods for handling uncertainty in GSC problems focus on SO, RO and DRO. However, aiming at the complex ambiguity of demand distribution, few studies handle it with a more flexible perspective of soft constraint.

Table 1
The summary of the related literature mentioned above.

Reference	Cooperation strategy		Uncertainty		Optimization method	Solution method
	Horizontal	Vertical	Demand	Cost		
You and Grossmann (2013)			✓		Stochastic	Benders decomposition
Saeed (2013)		✓			Deterministic	Commercial solver
Soysal et al. (2018)	✓		✓		Stochastic	Commercial solver
Kim et al. (2018)			✓		Robust	Commercial solver
Fan et al. (2020)	✓				Deterministic	Commercial solver
Tan et al. (2021)	✓				Deterministic	Heuristic
Hasani et al. (2021)				✓	Robust	Heuristic
Yazdekhasti et al. (2021)	✓	✓	✓		Stochastic	B&C
Hacardiaux and Tancrez (2022)	✓		✓		Stochastic	Commercial solver
Dong and Yuan (2025)			✓		Distributionally robust	Commercial solver
Petridis et al. (2023)				✓	Stochastic	Commercial solver
Elyasi et al. (2024)			✓		Stochastic	Heuristic
Wang et al. (2024a)			✓		Stochastic	Benders decomposition
Zhao et al. (2024)				✓	Distributionally robust	Commercial solver
Chen et al. (2024)			✓		Robust	Commercial solver
Our paper	✓		✓		GDRO	Customized B&C

- Solving complex models remains a significant challenge. Commercial solvers have been used in various studies, including Hacardiaux and Tancrez (2022), Dong and Yuan (2025), Petridis et al. (2023), Zhao et al. (2024), and Chen et al. (2024). In addition, some scholars have developed some algorithms to better suit specific problems, achieving higher solving efficiency. For instance, heuristic algorithms were used in Tan et al. (2021) and Elyasi et al. (2024), Benders decomposition in You and Grossmann (2013), Wang et al. (2024a), and B&C algorithm in Yazdekhasti et al. (2021). It is worth noting that among these customized algorithms, the exact solution algorithm performs better in solution quality, but there is insufficient attention given to the effective solving in the delivery of GSC.

This paper addresses the above research gaps by introducing a novel GDR-GSC model. The GDR-GSC model is designed to optimize production, transportation, and delivery decisions across multinational supply chain networks, incorporating horizontal cooperation strategies among distributors. This cooperation enables the sharing of customer information and coordination of vehicle routing, which reduces operational costs and improves supply chain resilience. The model integrates GDRO techniques, leveraging both inner and outer ambiguity sets to manage worst-case scenarios and mitigate the impact of demand fluctuations. We also propose a customized B&C algorithm to solve the GDR-GSC model, enhancing the computational efficiency and solution quality, particularly in large-scale problem instances. By dynamically adding strengthened k-path cuts, the algorithm significantly reduces computation time while preserving solution accuracy.

3. Model formulation

In this section, we present a GDR production–transportation–delivery model for a GSC, involving multiple manufacturers, retailers, warehouses, and customers in two countries.

3.1. Problem statement, assumption and notations

The global logistics system of Amazon is underpinned by a vast network of fulfillment centers. As a key example of horizontal cooperation in a tech-driven context, in many regions (such as Europe and North America), Amazon's warehouses share real-time information on inventory levels and customer demand, allowing for dynamic routing and load balancing (Fan et al., 2020). Horizontal cooperation within multinational corporations is prevalent due to interconnected warehouse networks that balance workloads and inventory (Hacardiaux and Tancrez, 2020), increased supply chain resilience against disruptions (Lotfi and Larmour, 2021), and centralized ownership that

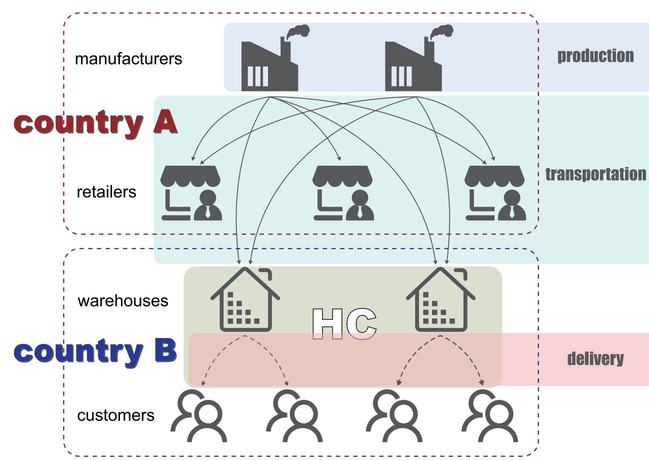

Fig. 1. GSC problem studied in this paper.

avoids profit-sharing hurdles faced by independent firms (Wen et al., 2019). Thus, this study integrates horizontal collaboration strategies among warehouses of a multinational corporation, coordinating vehicle scheduling across different warehouses under vehicle capacity constraints.

Specifically, we consider a GSC operated by a multinational corporation across two countries: Country A and B. The GSC is structured into four hierarchical tiers: manufacturers, retailers, warehouses, and end customers, as shown in Fig. 1.

- Manufacturers located in Country A are responsible for production, each with a predefined production capacity and incurring both startup and unit production costs.
- Retailers, also located in Country A, procure products from manufacturers at fixed wholesale prices and distribute them domestically. The transportation cost between manufacturers and retailers is a function of land-based distance.
- Warehouses, situated in Country B, receive goods shipped internationally from manufacturers. These warehouses incur both startup and operating costs, and serve as distribution hubs for the local market. A key modeling feature is the implementation of horizontal cooperation among warehouses. This enables the sharing of customer demand information and coordination of vehicle routing, thereby reducing logistical costs and improving responsiveness to demand fluctuations.
- End customers are located in Country B. Deliveries are executed using a fleet of vehicles with limited capacity, and the associated

Table 2
Notations.

Notation	Description
Sets	
$\mathcal{M} = \{1, 2, \dots, M\}$	Set of manufacturers in country A
$\mathcal{I} = \{1, 2, \dots, I\}$	Set of retailers in country A
$\mathcal{J} = \{1, 2, \dots, J\}$	Set of warehouses in country B
$\mathcal{K} = \{1, 2, \dots, K\}$	Set of customers in country B
$\mathcal{L} = \mathcal{J} \cup \mathcal{K}$	Set of nodes in country B
$\mathcal{V} = \{1, 2, \dots, V\}$	Set of vehicles used by warehouses
$\mathcal{N} = \{1, 2, \dots, N\}$	Set of sample data
Parameters	
C_m	Production capacity of manufacturer m
P_m	Startup cost of manufacturer m
G	Unit production cost
W^A_{mi}	Wholesale price from m to retailer i
W^B_{mj}	Wholesale price from m to warehouse j
TC	Unit land transportation cost
TS	Unit shipping cost
S^A_{mi}	Distance from m to retailer i
S^B_{mj}	Distance from m to warehouse j
R^A_i	Order quantity of retailer i
R^B_j	Order quantity of warehouse j
O_j	Operating cost of warehouse j
C_{jk}	Path cost for vehicle from j to k
VF	Fixed cost of using a vehicle
Q	Capacity of vehicle
d_k	Demand quantity of customer k
$X(\mathcal{S})/X^{\beta}(\mathcal{S})$	Sum/Affine sum of traffic flow entering the set $\mathcal{S}$
$\delta(\mathcal{S})$	All arcs crossing into or out of set $\mathcal{S}$
Decision variables	
q_m	Production quantity of manufacturer m
rt^A_{mi}	Quantity shipped from m to retailer i
rt^B_{mj}	Quantity shipped from m to warehouse j
Y^A_m	Binary variable for opening of manufacturer m
Y^B_j	Binary variable for opening of warehouse j
f_{jkv}	Binary variable for vehicle v traveling from j to k
u_{jv}	Position of node j in vehicle v's route
X_{jk}	Binary variable for customer k assigned to warehouse j

logistics are modeled as a vehicle routing problem, subject to routing feasibility constraints such as no repetition and subtour elimination (Quintero-Araujo et al., 2019).

The central objective of GSC problem is to jointly optimize production quantities, facility opening decisions, transportation flows, and delivery routes for a maximization of overall profit. The profit is from the total revenue derived from wholesale transactions minuses the aggregate costs related to production, transportation, warehousing, and distribution. For GSC problem, we have the following assumptions (Wang et al., 2021):

- The operational costs of warehouses are fixed and do not vary with the level of demand or the number of deliveries made.
- The wholesale prices of goods shipped from manufacturers to retailers and warehouses are fixed and determined by market conditions and agreements between the parties.
- The startup costs for opening a manufacturer or a warehouse are fixed and represent the one-time costs associated with initiating operations at these facilities.
- All vehicles used in the distribution process are assumed with same specification and type, which means they have identical operational cost.

We use the following sets, parameters, and variables to represent the elements and decisions of the GSC problem. All notations and symbols are shown in Table 2.

3.2. Deterministic GSC model

In this subsection, we present the mathematical model for the production–transportation–delivery problem in a GSC. The objective function aims to maximize the total revenue of the supply chain, while the constraints capture the various aspects of the production, transportation, and delivery processes.

$$\begin{aligned}\max \ & \sum_{m\in\mathcal{M}}\sum_{i\in\mathcal{I}} W^A_{mi} rt^A_{mi} - \sum_{m\in\mathcal{M}} Y^A_m P_m - \sum_{m\in\mathcal{M}} q_m G - \sum_{m\in\mathcal{M}}\sum_{i\in\mathcal{I}} S^A_{mi} rt^A_{mi} TC \\ & + \sum_{m\in\mathcal{M}}\sum_{j\in\mathcal{J}} W^B_{mi} rt^B_{mj} - \sum_{m\in\mathcal{M}}\sum_{j\in\mathcal{J}} S^B_{mj} rt^B_{mj} TS \\ & - \sum_{j\in\mathcal{L},k\in\mathcal{L},j\neq k}\sum_{v\in\mathcal{V}} f_{jkv} C_{jk} - \sum_{j\in\mathcal{J}} O_j Y^B_j - \sum_{j\in\mathcal{J}}\sum_{k\in\mathcal{K}}\sum_{v\in\mathcal{V}} f_{jkv} VF\end{aligned} \tag{1}$$

$$\text{s.t.} \quad q_m \le C_m Y^A_m, \quad \forall m \in \mathcal{M}; \tag{2}$$

$$q_m = \sum_{i\in\mathcal{I}} rt^A_{mi} + \sum_{j\in\mathcal{J}} rt^B_{mj}, \quad \forall m \in \mathcal{M}; \tag{3}$$

$$R_i = \sum_{m\in\mathcal{M}} rt^A_{mi}, \quad \forall i \in \mathcal{I}; \tag{4}$$

$$R_j = \sum_{m\in\mathcal{M}} rt^B_{mj}, \quad \forall j \in \mathcal{J}; \tag{5}$$

$$\sum_{j\in\mathcal{L}}\sum_{v\in\mathcal{V}} f_{jkv} = 1, \quad \forall k \in \mathcal{K}; \tag{6}$$

$$\sum_{k\in\mathcal{K}}\sum_{j\in\mathcal{L}} d_k f_{jkv} \le Q, \quad \forall v \in \mathcal{V}; \tag{7}$$

$$\sum_{k\in\mathcal{K}} d_k X_{jk} \le R_j Y^B_j, \quad \forall j \in \mathcal{J}; \tag{8}$$

$$\sum_{k\in\mathcal{L}} f_{jkv} - \sum_{k\in\mathcal{L}} f_{kjv} = 0, \quad \forall j \in \mathcal{L}, \forall v \in \mathcal{V}; \tag{9}$$

$$\sum_{j\in\mathcal{J}}\sum_{k\in\mathcal{K}} f_{jkv} \le 1, \quad \forall v \in \mathcal{V}; \tag{10}$$

$$u_{jv} - u_{kv} + Q f_{jkv} \le Q - d_k f_{jkv}, \quad \forall j \in \mathcal{K}, \forall k \in \mathcal{K}, \forall v \in \mathcal{V}, j \neq k; \tag{11}$$

$$\sum_{u\in\mathcal{K}} f_{juv} + \sum_{u\in\mathcal{L}\setminus k} f_{ukv} \le 1 + X_{jk}, \quad \forall j \in \mathcal{J}, \forall k \in \mathcal{K}, \forall v \in \mathcal{V}; \tag{12}$$

$$f_{jkv}, X_{jk}, D_j, Y^A_m, Y^B_j \in \{0,1\}, \quad \forall j \in \mathcal{J}, \forall k \in \mathcal{K}, \forall v \in \mathcal{V}, \forall m \in \mathcal{M}. \tag{13}$$

In this model, the objective function (1) aims to maximize the total revenue minus the total cost of the supply chain, whereinto the revenue includes the wholesale prices times quantities from the manufacturers to the retailers and warehouses, i.e., $\sum_{m\in\mathcal{M}}\sum_{i\in\mathcal{I}} W^A_{mi} rt^A_{mi}$ and $\sum_{m\in\mathcal{M}}\sum_{j\in\mathcal{J}} W^B_{mi} rt^B_{mj}$. The cost includes the start-up cost $\sum_{m\in\mathcal{M}} Y^A_m P_m$, production cost $\sum_{m\in\mathcal{M}} q_m G$, transportation cost $\sum_{m\in\mathcal{M}}\sum_{i\in\mathcal{I}} S^A_{mi} rt^A_{mi} TC$ and $\sum_{m\in\mathcal{M}}\sum_{j\in\mathcal{J}} S^B_{mj} rt_{mj} TS$ from the manufacturers to the retailers and warehouses, operation cost $\sum_{j\in\mathcal{J}} O_j Y^B_j$, path cost $\sum_{j\in\mathcal{L},k\in\mathcal{L},j\neq k}\sum_{v\in\mathcal{V}} f_{jkv} C_{jk}$ from the warehouses to the customers, and fixed cost $\sum_{j\in\mathcal{J}}\sum_{k\in\mathcal{K}}\sum_{v\in\mathcal{V}} f_{jkv} VF$ of using the trucks. The model is specifically governed by the following constraints: Constraints (2) indicate that manufacturers' production cannot surpass their capacity multiplied by their binary start-up variable. Constraints (3) assert that manufacturers' production equals to the aggregate of goods transported to retailers and warehouses. Constraints (4) and (5) signify that retailers' or warehouses' order quantity equals to the sum of goods transported from manufacturers. Constraints (6) stipulate that each customer can only be served once by one vehicle from one warehouse. Each vehicle's load must not exceed its capacity, as shown in constraints (7). Constraints (8) dictate that a warehouse's shipment cannot exceed its demand multiplied by its binary start-up variable. The inflow of each node must equal to its outflow, as described in constraints (9). Constraints (10) state that each vehicle can serve at most one customer. Constraints (11) prohibit repetition or sub-cycles in each vehicle's path. Constraints (12) mandate that each vehicle's path must be directly connected. Finally, all variables are non-negative, with some being binary.

3.3. Globalized distributionally robust GSC model

In the real world, customer demands fluctuate due to various factors such as market dynamics, economic changes, or unforeseen events so that they are usually uncertain. This paper models the ambiguity in demand distribution of customers, and employs a generalized distributionally robust optimization framework to balance the robustness and feasibility. By treating $\tilde{d}_k$ as uncertain, the model becomes more adaptable to realistic demand scenarios, thus enhancing the applicability of the proposed optimization model.

To address the ambiguity distribution of demand $\tilde{d}_k$, we employ a GDRO approach, which allows for a more comprehensive treatment of uncertainty while maintaining computational efficiency and model flexibility (Liu et al., 2023). GDRO is to integrate distribution uncertainty and model error into the distributionally robust optimization model at the same time. Specifically, on the one hand, the GDRO model requires that the robustness constraint strictly establish the probability distribution in the distribution uncertainty set, and on the other hand, for the probability distribution that is not in the distribution uncertainty set (i.e., the model error occurs), the robustness constraint is allowed to be violated to a certain extent, and the degree of violation is controlled by the model error tolerance level. In the GDRO method, the selection of ambiguity sets is crucial. The ambiguity sets are typically divided into two categories: moment-based and discrepancy-based (Lin et al., 2022). To make the distribution in the ambiguity set closer to the nominal distribution, we opt for a discrepancy-based ambiguity set utilizing 1-Wasserstein metric (Luo and Mehrotra, 2019). The Wasserstein distance is a metric that measures the dissimilarity between two probability distributions by the minimum cost of transporting mass from one distribution to another. Formally, the 1-Wasserstein distance $d_W(\cdot,\cdot)$ between two probability distributions $\mathbb{X}$ and $\mathbb{Y}$ defined on a space Ξ is given by:

$$d_W(\mathbb{X},\mathbb{Y}) := \inf_{\Pi\in Q(\mathbb{X},\mathbb{Y})}\left\{\int_{\Xi\times\Xi}\|x-y\|\Pi(\mathrm{d}x,\mathrm{d}y)\right\},$$

where $\Pi(\mathbb{X},\mathbb{Y})$ is the set of all joint distributions on $\Xi\times\Xi$ with marginals $\mathbb{X}$ and $\mathbb{Y}$, $x\in\mathbb{X}$ and $y\in\mathbb{Y}$ and $\|\cdot\|$ represents an arbitrary norm on $\mathbb{R}^K$.

The terminology of inner and outer ambiguity sets in the GDR-GSC model follows well-established conventions in robust optimization literature, tracing back to the foundational work on globalized robust optimization (Ben-Tal et al., 2017). This inner and outer ambiguity sets create a hierarchical protection mechanism: the inner ambiguity set $\mathcal{F}_W(\theta)$ defines the core region where constraints must be strictly satisfied (corresponding to high-probability demand scenarios), while the outer ambiguity set $\mathcal{P}(\Xi)$ encompasses a broader range of possible distributions (including low-probability extreme events). The Wasserstein distance-based formulation of these sets provides both mathematical rigor and practical interpretability, as it quantifies distributional differences in terms of optimal transport costs. The containment relationship ($\mathcal{F}_W(\theta)\subseteq\mathcal{P}(\Xi)$) inherently embodies varying levels of protection priority, enabling our model to strictly enforce constraint satisfaction for mandatory demand fulfillment scenarios while maintaining controlled adaptability when encountering statistically rare demand variations—an essential capability for supply chain risk mitigation.

The outer ambiguity set for uncertain demand vector $\tilde{\boldsymbol{d}}=(\tilde{d}_1,\tilde{d}_2,\dots,\tilde{d}_K)$ is defined as $\mathcal{P}(\Xi)$, which is the set of all possible probability distributions on the support set Ξ. Specifically, the support set Ξ defines the feasible region for demand realizations, containing all possible values of uncertain demand vector $\tilde{\boldsymbol{d}}$. Furthermore, the inner ambiguity set can be expressed as

$$\mathcal{F}_W(\theta)=\left\{\mathbb{P}\in\mathcal{P}(\Xi)\,:\,d_W\left(\mathbb{P},\hat{\mathbb{P}}\right)\le\theta\right\}, \tag{14}$$

where $\mathcal{F}_W(\theta)$ is the set of probability distribution $\mathbb{P}$ that has a Wasserstein distance at most θ from the empirical distribution $\hat{\mathbb{P}}$, with $\hat{\mathbb{P}}=\sum_{n\in\mathcal{N}}\delta_{\hat{d}_n}/N$. That is uniformly supported on N empirical realizations $\hat{\boldsymbol{d}}=(\hat{\boldsymbol{d}}_1,\dots,\hat{\boldsymbol{d}}_N)^T$.

In the global supply chain model, uncertain demand vector $\tilde{\boldsymbol{d}}$ is characterized through a hierarchical set framework following the GDRO method. The inner ambiguity set $\mathcal{F}_W(\theta)$ contains all probability distributions within a Wasserstein distance θ of the empirical distribution $\hat{\mathbb{P}}$, enforcing strict feasibility for high-probability demand. This is nested within the outer ambiguity set $\mathcal{P}(\Xi)$ encompassing all possible distributions on the support Ξ, which provides controlled flexibility for extreme demand realizations. The Wasserstein metric quantifies distributional deviations in terms of optimal transport costs, with θ serving as a tunable risk parameter—smaller values yield more conservative solutions for reliable demand trends, while larger values accommodate greater volatility. This dual-set structure creates a rigorous yet interpretable framework for demand uncertainty quantification, where the inner ambiguity set ensures robust constraint satisfaction while the outer ambiguity set maintains adaptability for critical demand variations.

Based on the outer ambiguity set $\mathcal{P}(\Xi)$ and inner ambiguity set (14), our GDR-GSC model can be reformulated as follows:

$$\begin{aligned}
\max\ & \sum_{m\in\mathcal{M}}\sum_{i\in\mathcal{I}}W^A_{mi}rt^A_{mi}-\sum_{m\in\mathcal{M}}Y^A_mP_m-\sum_{m\in\mathcal{M}}q_mG-\sum_{m\in\mathcal{M}}\sum_{i\in\mathcal{I}}S^A_{mi}rt^A_{mi}TC\\
&+\sum_{m\in\mathcal{M}}\sum_{j\in\mathcal{J}}W^B_{mi}rt^B_{mj}-\sum_{m\in\mathcal{M}}\sum_{j\in\mathcal{J}}S^B_{mj}rt^B_{mj}TS\\
&-\sum_{j\in\mathcal{L},k\in\mathcal{L},j\neq k}\sum_{v\in\mathcal{V}}f_{jkv}C_{jk}-\sum_{j\in\mathcal{J}}O_jY^B_j-\sum_{j\in\mathcal{J}}\sum_{k\in\mathcal{K}}\sum_{v\in\mathcal{V}}f_{jkv}VF
\end{aligned}$$

s.t. Constraints (2)–(6), (9)–(10), (12)–(13),

$$\mathbb{E}_{\mathbb{P}}\Big[\sum_{k\in\mathcal{K}}\sum_{j\in\mathcal{L}}\tilde{d}_kf_{jkv}-Q\Big]\le\gamma_1\min_{\mathbb{Q}\in\mathcal{F}_W(\theta)}d_W(\mathbb{P},\mathbb{Q}),\quad\forall\mathbb{P}\in\mathcal{P}(\Xi),\forall v\in\mathcal{V}, \tag{15a}$$

$$\mathbb{E}_{\mathbb{P}}\Big[\sum_{k\in\mathcal{K}}\tilde{d}_kX_{jk}-R_jY^B_j\Big]\le\gamma_2\min_{\mathbb{Q}\in\mathcal{F}_W(\theta)}d_W(\mathbb{P},\mathbb{Q}),\quad\forall\mathbb{P}\in\mathcal{P}(\Xi),\forall j\in\mathcal{J}, \tag{15b}$$

$$\mathbb{E}_{\mathbb{P}}\Big[u_{jv}-u_{kv}+Qf_{jkv}-Q+\tilde{d}_kf_{jkv}\Big]\le\gamma_3\min_{\mathbb{Q}\in\mathcal{F}_W(\theta)}d_W(\mathbb{P},\mathbb{Q}), \tag{15c}$$
$$\forall\mathbb{P}\in\mathcal{P}(\Xi),\forall v\in\mathcal{V},\forall j,k\in\mathcal{K},j\neq k.$$

Constraints (15a)–(15c) are GDRO constraints about demand, due to the ambiguity of distributions, these constraints cannot be enumerated, which means the GDR-GSC model is a semi-infinite system. For instance, constraints (15a) can be interpreted through two cases:

Case I: $$\mathbb{E}_{\mathbb{P}}\Big[\sum_{k\in\mathcal{K}}\sum_{j\in\mathcal{L}}\tilde{d}_kf_{jkv}-Q\Big]\le 0,\quad\forall\mathbb{P}\in\mathcal{F}_W(\theta),\forall v\in\mathcal{V},$$

wherein no constraint violations occur for any distribution within the ambiguity set $\mathcal{F}_w(\theta_1)$.

Case II: $$\mathbb{E}_{\mathbb{P}}\Big[\sum_{k\in\mathcal{K}}\sum_{j\in\mathcal{L}}\tilde{d}_kf_{jkv}-Q\Big]\le\gamma_1\min_{\mathbb{Q}\in\mathcal{F}_W(\theta)}d_W(\mathbb{P},\mathbb{Q}),$$
$$\forall\mathbb{P}\in\mathcal{P}(\Xi)\backslash\mathcal{F}_W(\theta),\forall v\in\mathcal{V},$$

where controlled violations (via tolerance parameter γ_1) for distributions in $\mathcal{P}(\Xi)\backslash\mathcal{F}_W(\theta)$ demonstrate soft outer robustness by bounding potential violations.

In these constraints, the right-hand side $\gamma_i\min_{\mathbb{Q}\in\mathcal{F}_W(\theta)}d_W(\mathbb{P},\mathbb{Q})$ serves as a violation budget, transforming them into soft constraints: when the distribution $\mathbb{P}$ is within the inner ambiguity set, the violation degree is minimal, enforcing strict compliance (hard constraint); as $\mathbb{P}$ moves to the outer ambiguity set with higher uncertainty, the violation degree expands, allowing controlled violation of the left-hand side expectation by an amount regulated by the tolerance parameter γ_i. Here, γ_i balances robustness and conservatism—larger values signify a more lenient attitude towards constraint violations and greater acceptance of uncertainty-related risks.

The proposed GDR-GSC model (15) makes decisions under the worst-case scenarios of the ambiguous demand, and provides robust and efficient solutions for the production–transportation–delivery problem. In the GDR-GSC model, constraints (15a)–(15c) are the GDR expectation constraints, and also are the key difficulties in solving the proposed model. They are semi-infinite constraints, and need to derive their tractable counterpart forms based on inner and outer distributional ambiguity sets. Therefore, in the subsequent section, we will look into the ways of transforming the GDR-GSC model into a more tractable form and explore the solution methods.

4. Model analysis

In this section, we analyze the properties and solution methods of the GDR model. We transform the GDR model into a more manageable form by eliminating the semi-infinite constraints.

4.1. Tractable GDR counterpart of expectation constraints

To address the GDR expectation constraints outlined in (15a)–(15c), we convert these semi-infinite constraints into some finite systems.

Theorem 1. *Suppose that Ξ is a box, i.e., $\Xi = \{\boldsymbol{d} \in \mathbb{R}^K : |d_k| \le \Lambda, k = 1,2,\ldots,K\}$. Let $\boldsymbol{f}_{jv} = (f_{j1v}, f_{j2v}, \ldots, f_{jKv})^T$ and $\boldsymbol{X}_j = (X_{j1}, X_{j2}, \ldots, X_{jK})^T$. Given the outer ambiguity set $\mathcal{P}(\Xi)$ and inner ambiguity set (14), by introducing auxiliary variables $\tau_n^i, s_n^i \in \mathbb{R}, \boldsymbol{\omega}_n^i \in \mathbb{R}^K, i = 1,2,3, \forall n \in \mathcal{N}$, we can obtain the following equivalent systems of constraints (15a)–(15c):*

$$
\begin{cases}
\theta N t^i + \sum_{n\in\mathcal{N}} s_n^i \le 0, i = 1,2,3, & (16a)\\
-Q + \hat{\boldsymbol{d}}_n^T \sum_{j\in\mathcal{K}} \boldsymbol{f}_{jv} + \boldsymbol{\omega}_n^1 \hat{\boldsymbol{d}}_n^T + \Lambda\tau_n^1 \le s_n^1, \forall n\in\mathcal{N}, \forall v\in\mathcal{V}, & (16b)\\
-R_j Y_j^B + \hat{\boldsymbol{d}}_n^T \boldsymbol{X}_j + \boldsymbol{\omega}_n^2 \hat{\boldsymbol{d}}_n^T + \Lambda\tau_n^2 \le s_n^2, \forall n\in\mathcal{N}, \forall j\in\mathcal{K}, & (16c)\\
u_{jv} - u_{kv} + Q f_{jkv} - Q + \hat{\boldsymbol{d}}_n^T \boldsymbol{f}_{jv} + \boldsymbol{\omega}_n^3 \hat{\boldsymbol{d}}_n^T + \Lambda\tau_n^3 \le s_n^3, & \\
\quad \forall n\in\mathcal{N}, \forall v\in\mathcal{V}, \forall j,k\in\mathcal{K}, j\ne k, & (16d)\\
\left\| \boldsymbol{\omega}_n^1 + \sum_{j\in\mathcal{L}} \boldsymbol{f}_{jv} \right\|_\infty \le t^1, \forall v\in\mathcal{V}, \forall n\in\mathcal{N}, & (16e)\\
\left\| \boldsymbol{\omega}_n^2 + \boldsymbol{X}_j \right\|_\infty \le t^2, \forall j\in\mathcal{L}, \forall n\in\mathcal{N}, & (16f)\\
\left\| \boldsymbol{\omega}_n^3 + \boldsymbol{f}_{jv} \right\|_\infty \le t^3, \forall j\in\mathcal{L}, \forall v\in\mathcal{V}, \forall n\in\mathcal{N}, & (16g)\\
\tau_n^i \ge \left\| \boldsymbol{\omega}_n^i \right\|_1, i = 1,2,3, \forall n\in\mathcal{N}, & (16h)\\
t^i \in [0, \gamma_i], i = 1,2,3. & (16i)
\end{cases}
$$

Proof. The proof of Theorem 1 is presented in Appendix. □

4.2. Linearization of constraints

The norm-based nonlinear terms in the constraints (16e)–(16h) directly affect the solution of the model. Thus, we will linearize the nonlinear constraints (16e)–(16h) by taking constraint (16e) as an example:

$$
\begin{aligned}
&\left\| \boldsymbol{\omega}_n^1 + \sum_{j\in\mathcal{L}} \boldsymbol{f}_{jv} \right\|_\infty \le t^1, \forall v\in\mathcal{V}, \forall n\in\mathcal{N}\\
\Rightarrow &\max_{\forall v\in\mathcal{V}, \forall n\in\mathcal{N}} \left| \boldsymbol{\omega}_n^1 + \sum_{j\in\mathcal{L}} \boldsymbol{f}_{jv} \right| \le t^1\\
\Rightarrow &\left| \boldsymbol{\omega}_n^1 + \sum_{j\in\mathcal{L}} \boldsymbol{f}_{jv} \right| \le t^1, \forall v\in\mathcal{V}, \forall n\in\mathcal{N}\\
= &\begin{cases}
\boldsymbol{\omega}_n^1 + \sum_{j\in\mathcal{L}} \boldsymbol{f}_{jv} \le t^1, \ if\ \boldsymbol{\omega}_n^1 + \sum_{j\in\mathcal{L}} \boldsymbol{f}_{jv} \ge 0, \ \forall v\in\mathcal{V}, \forall n\in\mathcal{N},\\
-\boldsymbol{\omega}_n^1 - \sum_{j\in\mathcal{L}} \boldsymbol{f}_{jv} \le t^1, \ if\ \boldsymbol{\omega}_n^1 + \sum_{j\in\mathcal{L}} \boldsymbol{f}_{jv} \le 0, \ \forall v\in\mathcal{V}, \forall n\in\mathcal{N}.
\end{cases}
\end{aligned}
$$

Similarly, constraints (16e)–(16g) can be replaced equivalently with the following constraints:

$$\boldsymbol{\omega}_n^1 + \sum_{j\in\mathcal{L}} \boldsymbol{f}_{jv} \le t^1, \forall v\in\mathcal{V}, \forall n\in\mathcal{N}, \tag{17}$$

$$-\boldsymbol{\omega}_n^1 - \sum_{j\in\mathcal{L}} \boldsymbol{f}_{jv} \le t^1, \forall v\in\mathcal{V}, \forall n\in\mathcal{N}, \tag{18}$$

$$\boldsymbol{\omega}_n^2 + \boldsymbol{X}_j \le t^2, \forall j\in\mathcal{L}, \forall n\in\mathcal{N}, \tag{19}$$

$$-\boldsymbol{\omega}_n^2 - \boldsymbol{X}_j \le t^2, \forall j\in\mathcal{L}, \forall n\in\mathcal{N}, \tag{20}$$

$$\boldsymbol{\omega}_n^3 + \boldsymbol{f}_{jv} \le t^3, \forall j\in\mathcal{L}, \forall v\in\mathcal{V}, \forall n\in\mathcal{N}, \tag{21}$$

$$-\boldsymbol{\omega}_n^3 - \boldsymbol{f}_{jv} \le t^3, \forall j\in\mathcal{L}, \forall v\in\mathcal{V}, \forall n\in\mathcal{N}. \tag{22}$$

For each component k of $\boldsymbol{\omega}_n^i$, introduce auxiliary variables $p_{n,k}^i$ and $q_{n,k}^i$ such that $\omega_{n,k}^i = p_{n,k}^i - q_{n,k}^i$, where $p_{n,k}^i \ge 0$, $q_{n,k}^i \ge 0$. Constraints (16h) can be transformed into the following linear equivalent form:

$$\tau_n^i \ge \sum_k (p_{n,k}^i + q_{n,k}^i), \ i = 1,2,3, \forall n\in\mathcal{N}, \tag{23}$$

$$\tau_n^i \ge p_{n,k}^i + q_{n,k}^i, \ i = 1,2,3, \forall k\in\mathcal{K}, \forall n\in\mathcal{N}, \tag{24}$$

$$\omega_{n,k}^i = p_{n,k}^i - q_{n,k}^i, \ i = 1,2,3, \forall k\in\mathcal{K}, \forall n\in\mathcal{N}, \tag{25}$$

$$p_{n,k}^i \ge 0, \quad q_{n,k}^i \ge 0, \ i = 1,2,3, \forall k\in\mathcal{K}, \forall n\in\mathcal{N}. \tag{26}$$

4.3. Equivalent formulation of GDR-GSC model

Based on Theorem 1, the original GDR expectation model (15) can be reformulated into the following equivalent model:

$$
\begin{aligned}
\max\ & \sum_{m\in\mathcal{M}}\sum_{i\in\mathcal{I}} W_{mi}^A rt_{mi}^A - \sum_{m\in\mathcal{M}} Y_m^A P_m - \sum_{m\in\mathcal{M}} q_m G - \sum_{m\in\mathcal{M}}\sum_{i\in\mathcal{I}} S_{mi}^A rt_{mi}^A TC\\
&+ \sum_{m\in\mathcal{M}}\sum_{j\in\mathcal{J}} W_{mi}^B rt_{mj}^B - \sum_{m\in\mathcal{M}}\sum_{j\in\mathcal{J}} S_{mj}^B rt_{mj}^B TS\\
&- \sum_{j\in\mathcal{L}, k\in\mathcal{L}, j\ne k}\sum_{v\in\mathcal{V}} f_{jkv} C_{jk} - \sum_{j\in\mathcal{J}} O_j Y_j^B - \sum_{j\in\mathcal{J}}\sum_{k\in\mathcal{K}}\sum_{v\in\mathcal{V}} f_{jkv} VF
\end{aligned} \tag{27}
$$

s.t. Constraints (2)–(6), (9)–(10), (12)–(13), (16a)–(16d), (16i), (17)–(26).

Solving the equivalent model (27) remains extremely challenging, since it is a MIP with VRP subproblem, so NP-hard (Kou et al., 2024). Therefore, in the next section, we will develop a B&C algorithm with specific strategies of branching and cut to handle it.

5. Customized B&C algorithm for GDR-GSC model

The B&C algorithm, a powerful technique that combines branch-and-bound with cutting-plane methods, is often used for solving mixed integer programming problems. To illustrate the overall logic, Pseudocode 1 on a standard B&C algorithm step is presented. However, the standard B&C algorithm fails to outperform general commercial solvers in solving our GDR-GSC model. Hence, there is a need for enhancements tailored to our specific problem within the standard B&C framework. In Section 5.1, we propose valid inequalities to expedite the algorithmic process. In Section 5.2, we analyze the branching strategy within the B&C algorithm and put forward specific branching strategies for our problem. In Section 5.3, we give a pseudocode of a customized B&C algorithm.

5.1. Strengthened k-path cuts for the GDR-GSC model

We introduce a strengthened k-path cut as valid inequality to reinforce the vehicle routing constraints. The intuition behind k-path cuts stems from the observation that for any subset $\mathcal{S} \subseteq \mathcal{K}$ of customer nodes, the total demand within this subset must be met by a sufficient number of vehicles, each with a limited capacity Q. Therefore, at least

Algorithm 1 Standard B&C Algorithm

```
Initialize problem with root node
Set lower bound LB ← −∞
Set upper bound UB ← +∞
Add root node to the queue Q
while Q is not empty do
    Select and remove node P from Q with best bound
    Solve the LP relaxation of P
    if LP is infeasible or LP bound ≥ UB then
        Discard node P
        continue
    end if
    if LP solution is integer feasible then
        if LP objective < UB then
            UB ← LP objective
            Store current solution as best
        end if
        continue
    end if
    Apply cutting planes (valid inequalities) to strengthen the relaxation
    Re-optimize the LP with cuts
    if LP becomes infeasible or bound ≥ UB then
        Discard node P
        continue
    end if
    Choose a branching variable
    Create child nodes P1 and P2 by branching
    Add P1 and P2 to Q
end while
return the best integer solution found
```

$\lceil \sum_{\mathcal{K}\in\mathcal{S}} d_k/Q \rceil$ vehicles must enter this subset. Denote the minimum number as $k(\mathcal{S})$, and the standard cutset inequality is

$$\sum_{v\in\mathcal{V}} \sum_{(j,k)\in\delta(\mathcal{S})} f_{jkv} \geq k(\mathcal{S}),$$

where $\delta(\mathcal{S})$ is the set of arcs crossing the boundary of subset $\mathcal{S}$, and f_{jkv} indicates whether vehicle v travels from node j to node k (Costa et al., 2019). To strengthen this inequality, we introduce weighting coefficients $\beta_{jkv} \in \{0,1\}$, where $\beta_{jkv} = 1$ if arc (j,k) is relevant to entering $\mathcal{S}$, and 0 otherwise. The strengthened k-path cut becomes

$$\sum_{v\in\mathcal{V}} \sum_{(j,k)\in\delta(\mathcal{S})} \beta_{jkv} f_{jkv} \geq k(\mathcal{S}). \tag{28}$$

A very intuitive method is given to estimate $k(\mathcal{S})$. We use the total demand of all customers in the set $\mathcal{S}$, divided by the capacity of vehicles, and take the upper bound, i.e.

$$k(\mathcal{S}) = \left\lceil \frac{d(\mathcal{S})}{Q} \right\rceil = \left\lceil \frac{\sum_{k\in\mathcal{S}} d_k}{Q} \right\rceil.$$

To concretely illustrate this concept, consider a small instance where customer subset $\mathcal{S} = \{k_1, k_2, k_3\}$ has demands $d_{k_1} = 800$, $d_{k_2} = 700$, $d_{k_3} = 1000$, and the vehicle capacity $Q = 1000$. Then the total demand in $\mathcal{S}$ is 2500, requiring at least $\lceil 2500/1000 \rceil = 3$ vehicles. If we identify three arcs entering this subset used by vehicles in the current solution, e.g., $f_{j_1k_1v_1}, f_{j_2k_2v_2}, f_{j_3k_3v_3}$, we can set $\beta_{jkv} = 1$ for these arcs and 0 elsewhere to enforce at least three vehicles cross into $\mathcal{S}$. This helps prune infeasible or weakly constrained solutions during the B&C process. Next up, we conduct a feasibility reasoning with four detailed steps.

Step 1: Total demand over subset $\mathcal{S}$

Let the total demand of customers in subset $\mathcal{S} \subseteq \mathcal{K}$ be

$$D(\mathcal{S}) := \sum_{k\in S} d_k.$$

Since each vehicle has a capacity Q, the minimum number of vehicles required to fulfill the demand is

$$k(\mathcal{S}) := \left\lceil \frac{D(\mathcal{S})}{Q} \right\rceil.$$

Step 2: Capacity-based necessity

Suppose a feasible solution employs vehicles to serve the customer set $\mathcal{S}$ fewer than $k(\mathcal{S})$, the total capacity of all vehicles entering or serving $\mathcal{S}$ will be less than

$$k(\mathcal{S})Q < D(\mathcal{S}).$$

This would make it impossible to deliver the required amount of goods to all customers in $\mathcal{S}$, contradicting feasibility. Therefore, any feasible solution must allocate at least $k(\mathcal{S})$ vehicles to serve $\mathcal{S}$.

Step 3: Link to arc-based formulation

Let $\delta(\mathcal{S})$ denote the set of arcs crossing into or out of $\mathcal{S}$, i.e.,

$$\delta(\mathcal{S}) := \{(j,k) \in \mathcal{J} \times \mathcal{S}\} \cup \{(k,j) \in \mathcal{S} \times \mathcal{J}\}.$$

Assume that every vehicle route is recorded by a binary variable f_{jkv}, indicating whether a vehicle v travels on arc (j,k). Then the number of vehicles entering or leaving $\mathcal{S}$ is given by

$$X(\mathcal{S}) := \sum_{v\in\mathcal{V}} \sum_{(j,k)\in\delta(\mathcal{S})} f_{jkv}.$$

We apply indicator coefficients $\beta_{jkv} \in \{0,1\}$ to restrict to a subset of arcs (e.g., only incoming ones, or filtered based on route structure)

$$X^{\beta}(\mathcal{S}) := \sum_{v\in\mathcal{V}} \sum_{(j,k)\in\delta(\mathcal{S})} \beta_{jkv} f_{jkv}.$$

By assumption, all deliveries must go through arcs in $\delta(\mathcal{S})$, and no delivery is possible without a path in this set. Thus,

$$X^{\beta}(\mathcal{S}) \geq X(\mathcal{S}) \geq k(\mathcal{S}).$$

Step 4: Conclusion

Therefore, the inequality

$$\sum_{v\in\mathcal{V}} \sum_{(j,k)\in\delta(\mathcal{S})} \beta_{jkv} f_{jkv} \geq \left\lceil \frac{\sum_{k\in\mathcal{S}} d_k}{Q} \right\rceil$$

is a valid inequality for all feasible solutions of the GDR-GSC model, and thus constitutes a strengthened k-path cut that tightens the feasible region of the integer programming formulation.

Strengthened k-path cuts enhance constraints on the solution by limiting the number of vehicle paths in the solution. The introduction of cuts helps to more precisely describe the overall structure of the problem, improving the tightness of upper and lower bounds in the linear programming relaxation problem. By introducing strengthened k-path cuts, we aim to refine the algorithm's performance, making it more effective in solving GDR-GSC by providing more compact bounds and optimized solutions.

5.2. Joint branching strategy for the GDR-GSC model

This subsection focuses on the branching strategy within the B&C algorithm, tailored specifically for solving the GDR-GSC model. The branching strategy is a critical component of the B&C framework, as it determines how the solution space is explored by partitioning it into smaller subproblems. Some generic strategies like most-fractional (MF) branching (Ortega and Wolsey, 2003), strong branching (Dey et al., 2024), and pseudocost branching (Seman et al., 2023), are often utilized in B&C algorithm. However, due to the high dimensionality and structural complexity of our model, especially the vehicle routing subproblem under uncertainty, these conventional strategies are inefficient. Therefore, a joint branching strategy that combines SOS branching (De Farias et al., 2008) with PSP branching (Beale and Forrest, 1976) is designed and customized for the characteristics of the GDR-GSC problem.

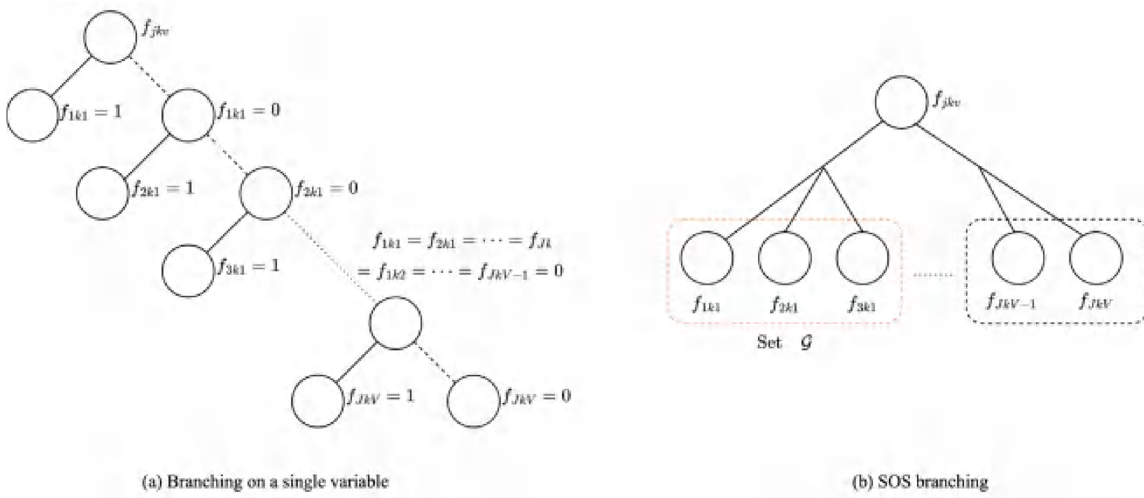

Fig. 2. SOS branching strategy for the GDR-GSC model.

In our model, the key binary variable f_{jkv} indicates whether vehicle v travels from node j to node k. Because each customer $k \in \mathcal{K}$ must be served exactly once by a single vehicle, a classical SOS constraint is structured as $\sum_{j\in\mathcal{L}}\sum_{v\in\mathcal{V}} f_{jkv} = 1$, which ensures for each customer, only one variable in the set $\{f_{jkv}\}_{j\in\mathcal{L},k\in\mathcal{K},v\in\mathcal{V}}$ can equal to 1 while the rest are zero. Once SOS branching is satisfied, we can efficiently partition the feasible region by selecting a subset of variables (e.g., routes for a particular customer) and creating branches based on prioritization rules rather than branching on individual variables. To implement this, we define a set $\mathcal{G} \subseteq \mathcal{L}\times\mathcal{V}$ based on fractional values of f_{jkv} in the current solution, then prioritize exploration of nodes in $\mathcal{G}$ using the following formulas:

$$\mathcal{G} := \{(j,v) \in \mathcal{L}\times\mathcal{V} \mid j \le \alpha_1, v \le \alpha_2\} \text{ with } \alpha_1 := \sum_{j\in\mathcal{L}} f_{jkv}\, j \text{ and } \alpha_2 := \sum_{v\in\mathcal{V}} f_{jkv}\, v.$$

Here, α_1 and α_2 are weighted averages that reflect the fractional influence of each variable in the candidate set, guiding the branching process towards the most promising nodes. As depicted in Fig. 2, the SOS branching scheme shows it has significantly advantageous than the standard way of doing branching on a single variable for each instance. This leads to a notable reduction in the number of nodes in the branch-and-bound tree.

Following the SOS-based partitioning, we further refine the search using PSP branching. This technique leverages information from dual variables (shadow prices) to prioritize variables whose branching is expected to lead to the greatest improvement in the objective function. By integrating these two strategies: structural SOS branching for routing constraints and PSP branching for other variables, we ensure both global convergence and local efficiency.

To highlight the efficiency of the joint branching strategy, a set of experiments is conducted. In the experimental setup with k-path cutting as the cut plane, we compare the PSP branching, SOS branching, MF branching, and joint branching strategy (PSP&SOS). Keeping other parameters fixed, the final results of the compute time (CPU(s)) and compute nodes (Nodes) are presented in Table 3. Several important observations can be drawn regarding the performance of different branching strategies in the customized B&C algorithm for the GDR-GSC model. (*i*) The GDR-GSC model cannot be solved using the SOS branching strategy alone. (*ii*) The joint branching strategy, which combines SOS and PSP branching, consistently outperforms the other strategies – MF branching, standalone SOS branching, and PSP branching – across all tested instances. Specifically, in terms of computational time, the joint strategy achieves the shortest solution times in every instance. (*iii*) Furthermore, the joint strategy leads to a substantial reduction in the number of explored branch-and-bound nodes, which reflects a more efficient search process and tighter relaxation bounds. For example, when the number of customers increases to 13, the joint strategy reduces the node count by more than 30% compared to the next-best strategy.

Notably, the PSP and MF branching strategies can produce feasible results individually, the SOS branching strategy alone fails to work within the B&C framework. Specifically, it is unable to generate a complete branch-and-bound tree and thus does not yield any valid solution, indicating that SOS branching in isolation is insufficient for solving the GDR-GSC model. In smaller problem sizes, all strategies perform comparably; However, as the problem size grows, the advantages of the PSP&SOS branching strategy become increasingly significant, demonstrating superior scalability. This suggests that the joint strategy not only accelerates convergence but also improves the tractability of solving large-scale mixed-integer nonlinear problems under uncertainty. These results validate the effectiveness of the proposed branching mechanism in reducing computational burden while preserving or even improving solution quality.

5.3. Pseudocode of customized B&C algorithm

The customized B&C algorithm that incorporates strengthened k-path cuts and joint branching strategy can improve the efficiency of solving large scale mixed-integer programming. The key algorithmic steps are summarized and outlined as follows:

Step 1 Initialization

Set initial lower and upper bounds (LB, UB). Add the root node (original GDR-GSC problem) to the priority queue Q.

Step 2 LP Relaxation and Feasibility Check

While Q is not empty:

•Select the node P with the best bound;

•Solve its LP relaxation;

•If the solution is infeasible or worse than UB, discard P;

•If the solution is integer feasible and better than UB, update UB and save the solution.

Step 3 Branching and Cutting

If the solution is not integer feasible:

•Apply joint branching: first SOS branching (for routing constraints), then PSP branching (guided by shadow prices);

Table 3
Performance comparison of different branching strategies for the GDR-GSC model.

Instance	MF		PSP		SOS		PSP&SOS	
	CPU(s)	Nodes	CPU(s)	Nodes	CPU(s)	Nodes	CPU(s)	Nodes
$\mathcal{K} = 8$	1.5	36 428	1.2	25 673	–	–	0.9	21 506
$\mathcal{K} = 9$	6.1	160 485	5.6	157 834	–	–	4.8	137 059
$\mathcal{K} = 10$	53.8	1 398 475	40.5	1 037 534	–	–	32.9	884 628
$\mathcal{K} = 11$	342.3	4 374 853	255.4	3 974 583	–	–	213.0	3563363
$\mathcal{K} = 12$	463.7	4 857 383	432.3	4 255 637	–	–	334.5	3875821
$\mathcal{K} = 13$	1987.5	10 995 110	1728.2	10 485 760	–	–	1450.3	9567453
Average	475.8	3 637 122	410.5	3 322 837	–	–	339.4	3008305

"–" indicates that the optimal value of the objective could not be acquired within the set time limit.

•Add strengthened k-path cuts to tighten the feasible region;

•Re-optimize the LPs of the new subproblems.

Step 4 Queue Update and Termination

•Add promising subproblems back into Q;

•Repeat until Q is empty;

•Return the best integer solution found.

Algorithm 2 below is the pseudocode for the B&C algorithm tailored for the GDR-GSC model.

Algorithm 2 Customized B&C Algorithm for GDR-GSC Model

```
Initialize the problem with the GDR-GSC model
Set the initial lower bound LB ← −∞
Set the initial upper bound UB ← +∞
Create an empty priority queue Q for storing subproblems
Add the root node (representing the original problem) to Q
while Q is not empty do
    Select and remove the subproblem P from Q with the lowest bound
    Solve the linear relaxation of P
    Let z^LP be the optimal value of the linear relaxation
    if z^LP ≥ UB then
        Discard subproblem P
        continue
    end if
    if P is integer feasible then
        if z^LP < UB then
            UB ← z^LP
            Store the current solution as the best found solution
        end if
        continue
    end if
    Apply the SOS branching strategy to create two new subproblems P_1 and P_2
    Apply PSP branching on P_1 and P_2 to further explore nodes
    Apply valid inequalities (strengthened k-path cuts) to P_1 and P_2
    Compute the bounds for P_1 and P_2
    if bound of P_1 < UB then
        Add P_1 to Q
    end if
    if bound of P_2 < UB then
        Add P_2 to Q
    end if
end while
return the best found solution
```

6. Numerical experiments

In this section, the performance of a customized B&C algorithm is first analyzed by a testing experiment. Next up, a realistic case is conducted to validate the proposed model and algorithm. All experiments are conducted on a machine running Linux 64-bit operating system with an Intel(R) Xeon(R) Silver 4116 CPU @ 2.10 GHz, using Gurobi 11.0.1 and Python 3.11 software.

Table 4
The number of warehouses and customers used in numerical experiments.

$\mathcal{J} \setminus \mathcal{K}$	8	9	10	11	12	13	14	15
2	✓	✓	✓	✓	✓			
3			✓	✓	✓	✓	✓	
4					✓	✓	✓	✓

6.1. Numerical examples

In this subsection, we use multiple numerical experiments to validate the effectiveness and superior performance of the customized B&C algorithm. If the optimal value obtained directly by the customized B&C algorithm and solver are the same, we consider the algorithm feasible. Then, we use the computation time to judge the superiority of the method. After verification, we find that the number of warehouses and customers has the most significant impact on the solution time and convergence speed. Therefore, we gradually increase the number of warehouse and customer nodes, and then compare the solution time and solution quality of the GDR-GSC model with and without the B&C algorithm. The number of warehouses and customers used in our experiments is shown in Table 4. Exploration of the enumeration tree is limited to 172,800s of CPU time. We preprocess a set of data for the experiments, with a portion of it being randomly generated by the dedicated program including demand d_k, warehouse opening cost O_j and distance S^A_{mi} and S^B_{mj}. The distance data refers to the distance between cities in China. The detailed data are shown in Table 5.

The detailed results of the numerical experiments, as presented in Table 6, clearly demonstrate the effectiveness and superiority of the customized B&C algorithm in solving the GDR-GSC model. In Table 6, "B&C" indicates the use of our customized B&C algorithm for solving. We dynamically add strengthened k-path cuts using the Gurobi solver's callback function. "BD" refers to solving the model using Benders decomposition algorithm. "Gurobi" indicates solving in the solver's default settings. The "Obj" column displays the optimal objective value obtained within the specified time limit. The "Gap(%)" column shows the relative gap of the current result as Gap $= \frac{|\text{ObjBound}-\text{ObjVal}|}{|\text{ObjVal}|}$. Wherein, ObjVal is the objective function value from the current solution, and ObjBound is an estimated bound (upper for minimization, lower for maximization) on the optimal objective value, used to calculate the gap. The "CPU(s)" column displays the solution time. Instances with solution times marked with "-" indicate that the optimal objective value could not be obtained within the specified time limit.

Specifically, (i) the algorithm consistently achieves the same optimal objective value as Gurobi solver across all tested problem sizes, confirming its correctness and feasibility. (ii) In terms of computational time, the customized B&C algorithm significantly outperforms Gurobi

Table 5
Data summary for the numerical experiments.

Parameters	Notations	Values	Unit	References
Manufacturing plants	$\mathcal{M}$	3		
Retailers	$\mathcal{I}$	23		
Vehicles	$\mathcal{V}$	3		
Production capacity for each m	C_m	20,000		Li et al. (2023)
Vehicle capacity	Q	4,000		Li et al. (2023)
Demand of customer k	d_k	$[700, 800]$		Li et al. (2023)
Wholesale price for m to i	W^A_{mi}	4.18	USD	Shanghai Oil & Gas Trading Center[a]
Wholesale price for m to j	W^B_{mj}	6.97	USD	Shanghai Oil & Gas Trading Center[a]
Startup cost for each m	P_m	139.32	USD	Li et al. (2023)
Unit manufacturing cost	G	1.93	USD	Li et al. (2023)
Unit transport cost for m to i	TC	0.03	USD	Commodity Price Network[b]
Unit transport cost for m to j	TS	0.02	USD	Commodity Price Network[b]
Route cost	VF	27.86	USD	Li et al. (2023)
Warehouse opening cost for each j	O_j	$[5.57, 11.15]$	USD	Li et al. (2023)
Distance from m to i	S^A_{mi}	$[30, 100]$	km	Google Maps[c]
Distance from m to j	S^B_{mj}	$[100, 200]$	km	Google Maps[c]
Radius of ambiguity set	θ	0.5		Liu et al. (2023)
Tolerance level	γ	0.5		Liu et al. (2023)

[a] https://www.shpgx.com/html/ChnLNGIndex.html
[b] https://price.mofcom.gov.cn/price_2021/trafficgoods/moretrafficgoods.shtml?flag=ly&w_m_y=week
[c] www.google.com/maps

Table 6
Comparison between B&C algorithms with Benders decomposition and Gurobi.

Instance		B&C			BD			Gurobi		
		Obj	Gap(%)	CPU(s)	Obj	Gap(%)	CPU(s)	Obj	Gap(%)	CPU(s)
$\mathcal{J}=2$	$\mathcal{K}=8$	382 239.2	0.0000	0.9	382 239.2	0.0000	2.1	382 239.2	0.0000	2.3
	$\mathcal{K}=9$	382 013.7	0.0000	4.8	382 013.7	0.0000	6.5	382 013.7	0.0000	7.7
	$\mathcal{K}=10$	382 065.0	0.0000	7.1	382 065.0	0.0000	23.5	382 065.0	0.0098	26.8
	$\mathcal{K}=11$	433 067.3	0.0091	32.9	433 067.3	0.0095	323.8	433 067.3	0.0095	292.4
	$\mathcal{K}=12$	433 090.2	0.0099	213.0	433 090.2	0.0100	315.8	433 090.2	0.0100	294.2
$\mathcal{J}=3$	$\mathcal{K}=10$	481 542.8	0.0041	13.4	481 542.8	0.0096	76.3	481 542.8	0.0096	61.9
	$\mathcal{K}=11$	481 304.7	0.0050	334.5	429 847.2	12.2436	846.7	481 304.7	0.0096	524.1
	$\mathcal{K}=12$	481 069.0	0.0099	3022.8	408 673.3	16.6438	11 365.8	481 069.0	0.0100	7493.8
	$\mathcal{K}=13$	481 046.5	0.0100	33 466.2	–	–	–	481 046.5	0.0100	57 244.8
	$\mathcal{K}=14$	480 920.3	0.0100	166 389.5	–	–	–	–	–	–
$\mathcal{J}=4$	$\mathcal{K}=12$	532 708.1	0.0100	2994.2	458 946.2	15.8734	10 783.5	532 708.1	0.0100	6115.6
	$\mathcal{K}=13$	532 582.3	0.0100	23 576.0	–	–	–	532 582.3	0.0100	34 242.0
	$\mathcal{K}=14$	532 676.1	0.0100	17 809.4	–	–	–	532 676.1	0.0100	27 156.6
	$\mathcal{K}=15$	532 497.2	0.0100	144 216.6	–	–	–	–	–	–
Average			0.0071	28 005.8		4.9767	63 410.3		0.0082	34 218.7

"–" indicates that the optimal value of the objective could not be acquired within the set time limit.

in larger-scale instances. For example, when the number of customer nodes increases from 8 to 15 and warehouse nodes increase from 2 to 4, Gurobi often reach its time limit of 172,800 s without producing an optimal solution, especially when customer nodes exceed 13. In contrast, the customized B&C algorithm is able to find optimal or near-optimal solutions in a substantially shorter time frame, highlighting its computational efficiency and scalability. (*iii*) Furthermore, the experiments reveal a critical limitation of standard Benders decomposition algorithm. While Benders could solve small- to medium-sized instances effectively, it fails to provide results for larger instances due to convergence issues and excessive memory or time consumption. Specifically, Benders decomposition becomes infeasible or terminated prematurely when the number of customers and warehouses increases beyond a certain threshold, indicating poor scalability for complex global supply chain problems with ambiguity.

In conclusion, the customized B&C algorithm not only maintains high solution quality but also demonstrates superior solving efficiency and robustness compared to both the default solver and Benders decomposition algorithm. It proves to be more scalable and reliable for handling large-scale, mixed-integer nonlinear optimization problems under demand ambiguity. These findings underscore the practical applicability of the proposed method in real-world global supply chain scenarios, particularly when computational resources and time are critical constraints.

6.2. Empirical study on Apple Inc.

In this subsection, we show a case study on the product sales of Apple in a particular quarter.

6.2.1. Background and data

Apple's strategy of establishing assembly factories in various parts of China is aimed at leveraging local labor and resources to meet global demand more efficiently. The Shenzhen manufacturer, as one of these facilities, holds a significant position in production, particularly in fulfilling the demands of both domestic and Southeast Asian markets. We will use the supply chain from the Shenzhen manufacturer to Guangdong Province and Malaysia as a case study. Guangdong Province

Table 7
Data utilized in the empirical study.

Parameters	Notations	Values	Unit
Manufacturing plants	$\mathcal{M}$	1	
Retailers	$\mathcal{I}$	21	
Vehicles	$\mathcal{V}$	4	
Production capacity for each m	C_m	1,000,000	
Vehicle capacity	Q	20,000	
Demand of customer k	d_k	$[10,000, 21,000]$	
Wholesale price for m to i	W^A_{mi}	700	USD
Wholesale price for m to j	W^B_{mj}	700	USD
Startup cost for each m	P_m	1,000	USD
Unit manufacturing cost	G	432	USD
Unit transport cost for m to i	TC	0.005	USD
Unit transport cost for m to j	TS	0.002	USD
Route cost	VF	1,250	USD
Warehouse opening cost for each j	O_j	3,000	USD
Radius of ambiguity set	θ	0.5	
Tolerance level	γ	0.5	

has 21 cities, and the West Malaysian Peninsula has 11 states and 2 federal territories.

The data utilized in the empirical study are introduced as follows:

- Customer demand (d_k), unit transportation costs (TC, TS), wholesale prices (W^A_{mi}, W^B_{mj}), and the number of vehicles are provided from Apple's Q1 2019 report.[1] We utilize the sales data from Malaysian retail outlets over the past five quarters as empirical distribution data for sales point demand. The numbers and locations of manufacturing plants and retailers are also obtained from this report. The above data are presented in Table 7.
- Referring to Quintero-Araujo et al. (2019), we obtain the production capacity (C_m), vehicle capacity (Q), vehicle route cost (VF), warehouse operating costs (O_j), facility startup cost (P_m), and unit production cost (G). The data mentioned above are also summarized in Table 7.
- One Apple sales point is select as end customer in every state and federal territory. The Malaysian Peninsula has four distributors, each with their own warehouse (W1 to W4) to receive products from the Shenzhen manufacturer and distribute them to sales points in each state and federal territory. The locations of customers and warehouses, along with the distance between facility points, are sourced from Google Maps.[2] The locations of warehouses and retailers are shown in Fig. 3, and the distances from the manufacturer to each retailer and warehouse are shown in Table 8.

The proposed case is in accordance with our GDR-GSC framework, and the customized B&C algorithm presented in Section 5 is employed for its resolution.

6.2.2. Computational result

In this subsection, a comprehensive discussion and completion regarding the calculation results of the GDR-GSC model are presented under specific parameter settings. Specifically, we consider the case where the ambiguity set parameter θ and the globalized sensitivity parameter γ are 0.5, and Λ equals to 1. The optimal profit value achieved is determined to be 2.408×10^8 dollars. This figure serves as a crucial benchmark for evaluating the economic viability and effectiveness of the modeled system. Moreover, with respect to the production aspect, it is found that the Shenzhen manufacturer has produced 990,000 units of products. This quantity provides insights into the production capacity and output level of the specific manufacturer within the overall supply

Table 8
The distance from manufacturer (Shenzhen) to retailers and distributors' warehouse (km).

Retailers	Distance	Retailers	Distance
Shantou	283.5	Huizhou	73.2
Chaozhou	290.3	Dongguan	59.8
Jieyang	261.6	Qingyuan	162.2
Meizhou	285.4	Guangzhou	105.6
Heyuan	148.5	Foshan	110.8
Retailers	Distance	Retailers	Distance
Zhaoqing	173.3	Yangjiang	227.4
Yunfu	211.6	Maoming	339.1
Jiangmen	101.8	Zhanjiang	408.4
Zhongshan	67.8	Shanwei	255.6
Zhuhai	57.9	Shaoguan	255.8
Warehouse	Distance	Warehouse	Distance
W1	2261.1	W3	2389.6
W2	2330.3	W4	2505.5

Table 9
Optimal allocation results form warehouses to customers.

Warehouse	Customers
W1	Ipoh ⇒ George Town⇒ Alor Setar ⇒ Kangar
W2	Kuala Lumpur ⇒ Shah Alam ⇒ Kota Baharu ⇒ Kuala Terengganu
W3	–
W4	Johor Baharu ⇒ Kota Melaka ⇒ Seremban ⇒ Putrajaya ⇒ Kuantan

chain framework. The quantity shipped from Shenzhen to each retailer in the country is 30,000, and the quantity shipped to the warehouses of various distributors in Malaysia is 90,000 respectively. Due to the fact that there exists only one manufacturer in Shenzhen, the demand of each retailer and warehouse in this context essentially corresponds to the transportation volume of products. This relationship simplifies the analysis of the product flow from the manufacturing source to the downstream distribution nodes.

Finally, we focus on the decisions related to the logistics and distribution operations in Malaysia. The customers-to-warehouse allocation decisions in Malaysia are all presented in Table 9. Specifically, different warehouses are assigned distinct distribution tasks. Warehouse "W1" is tasked with distributing products to customers located in the areas of Kangar, Alor Setar, George Town, and Ipoh. Warehouse "W2" is responsible for distributing to customers in Kuala Terengganu, Kota Baharu, Shah Alam, and Kuala Lumpur. Notably, Warehouse "W3" is not involved in the delivery process, which is due to the consideration of horizontal cooperation strategy to reduce costs. Warehouse "W4", on the other hand, is in charge of distributing to customers in Kuantan, Putrajaya, Seremban, Kota Melaka, and Johor Baharu.

7. Analysis and comparison

7.1. Parameter analysis and managerial insight

The impact of two ambiguity parameters, i.e., Wasserstein radius θ and tolerance level γ, on the GDR-GSC model is discussed. We conduct the experiments under different parameter combinations. First, the change trend of the optimal values is examined with respect to γ under the values of θ fixed as 0.1, 0.3, 0.5, 0.7, and 0.9, respectively. Fig. 4 indicates that as the tolerance level γ increases, the total revenue in the GDR-GSC model always shows an upward trend under various scenarios of θ. The finding reflects that the increase of tolerance level widens the distance between the inner and outer ambiguity sets, thereby relaxing constraints and providing decision makers with a broader feasible region, and finally optimizing economic objective.

Subsequently, when θ varies, the change trend of the optimal values is investigated with the values of γ fixed as 0.1, 0.3, 0.5, 0.7, and 0.9,

[1] www.apple.com/newsroom/2019/01/apple-reports-first-quarter-results
[2] www.google.com/maps

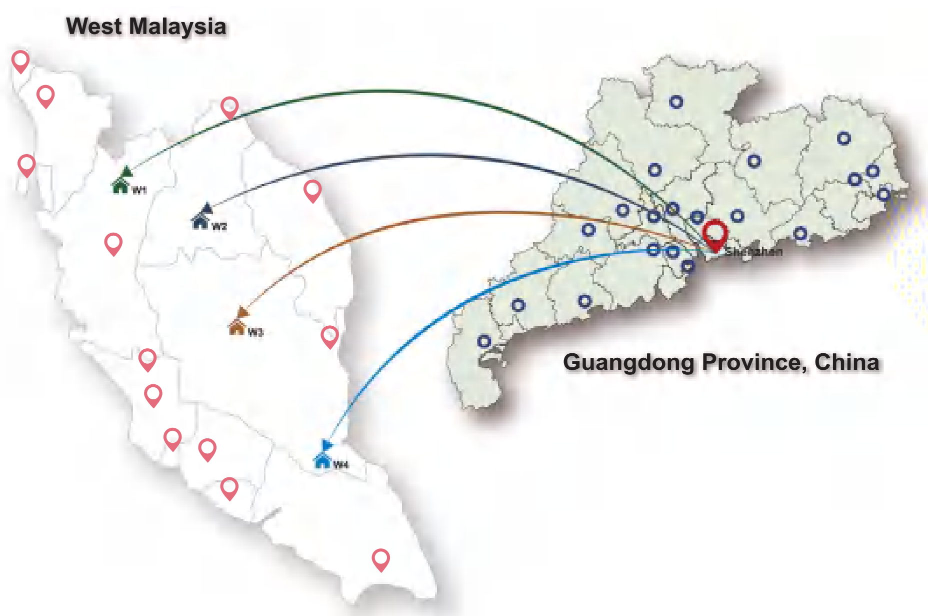

Fig. 3. The locations of warehouses, retailers, and customers in the empirical study.

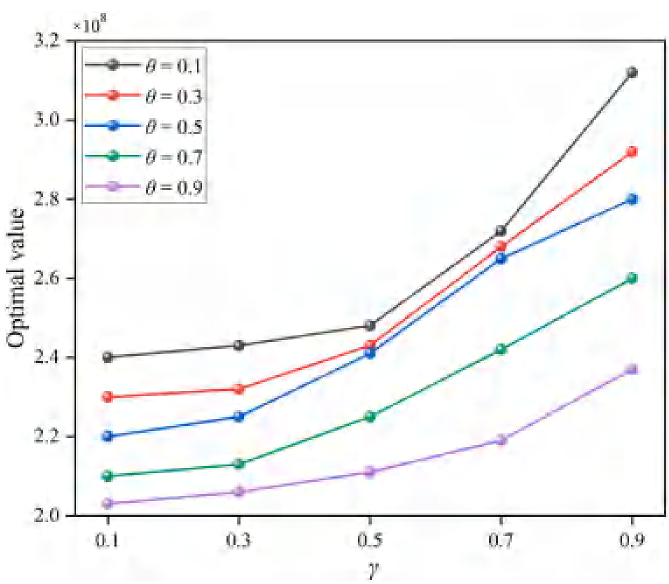

Fig. 4. The impact of tolerance level on the optimal value.

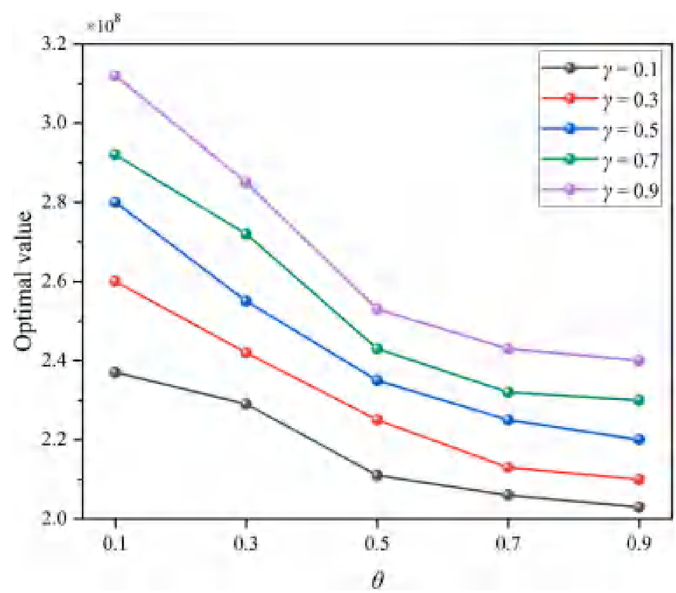

Fig. 5. The impact of Wasserstein radius on the optimal value.

respectively. Fig. 5 showcases that as the radius θ increases, the total revenue in the GDR-GSC model always shows a downward trend under various scenarios of γ. These results indicate that when Wasserstein radius increase, the revenue objective is getting smaller. The reason for this is that inner Wasserstein ambiguity set becomes larger. The range of the constraint to meet the complete feasibility is expanded, then decisions is more conservative and further deteriorate the revenue objective.

- **Analysis on tolerance level parameter** γ : The parameter γ is a tolerance level that controls the trade-off between robustness and conservatism in the GDRO approach. It allows for controlled constraint violation for distributions outside the ambiguity set. Since a larger violation of constraints implies a larger feasible region, the optimal value in the maximized objective will be greater. In practical terms, setting γ involves a strategic decision. A company might choose a higher γ if it values adaptability and cost-efficiency, even if it means risking some level of constraint violation during extreme events. Alternatively, a lower γ would be selected if the company prioritizes reliability and guarantee, aiming to minimize the impact of ambiguity on its supply chain operations.
- **Analysis on radius of ambiguity set** θ: The parameter θ defines the radius of the Wasserstein ambiguity set in the GDRO approach, which represents the level of ambiguity considered in the model. A larger θ indicates a broader set of possible demand distributions, thus capturing a higher level of ambiguity. This can lead to a more conservative optimization, which aims to ensure robustness against a wider range of scenarios. Because the larger ambiguity set, the more severe the worst-case scenario faced. In the context of maximizing, this typically results in a smaller

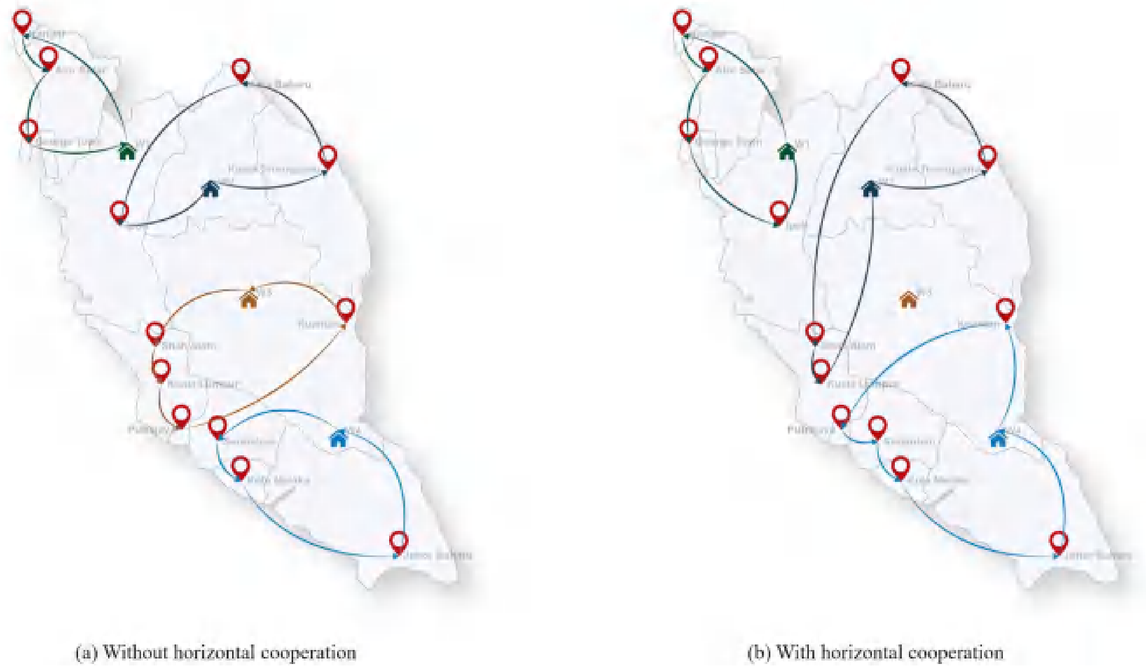

Fig. 6. Delivery routes of vehicles with and without horizontal cooperation.

optimal value. Conversely, a smaller θ results in a narrower ambiguity set, focusing on a more limited set of potential demand distributions. This may lead to a less conservative optimization process, while also increasing the risk. In the context of the GDR-GSC model, increasing θ would mean that the model is prepared to handle more variability in demand, which could be crucial in volatile markets. However, this increased robustness might come at the cost of higher operational expenses due to over-preparation for a wide range of scenarios. On the other hand, a smaller θ could result in cost savings but with the risk of being unprepared for unexpected shifts in demand.

- **Managerial insights**: The above findings provide the managerial insights to decision-makers in the following four aspects:
(1) Dynamically adjust uncertainty response strategies: In the model, the ambiguity set radius parameter θ and the global sensitivity parameter γ have a significant impact on the optimal profit. Specifically, an increase in θ (i.e., higher ambiguity in demand distribution) leads to a decrease in the optimal value, while an increase in γ (i.e., higher tolerance for constraint violations) results in an increase in the optimal value. This suggests that managers need to dynamically adjust strategies according to market volatility—in periods of stable demand, parameter θ can be reduced to lower the conservatism of decisions and thereby improve profits; in periods of market turbulence, θ should be increased to enhance supply chain resilience, and at the same time, parameter γ can be adjusted to balance risks and returns.
(2) Optimize warehouse and distribution resource allocation: The calculation results show that the horizontal cooperation strategy causes warehouse W3 in Malaysia to cease operations, and its originally served customers are reassigned to warehouses W2 and W4, reducing logistics costs through route integration. This indicates that multinational enterprises should promote information sharing and resource collaboration among warehouses at the same level, improve efficiency by merging redundant warehouse nodes and optimizing distribution routes. Especially in regions with scattered or highly fluctuating demand, this approach can significantly reduce transportation costs and improve the profit.
(3) Data-driven parameter calibration: The quantification of demand ambiguity relies on historical data (such as quarterly sales data of Apple retail stores in Malaysia in the case) to construct empirical distributions. Therefore, managers should attach importance to data accumulation and analysis, optimize the value of θ by continuously updating demand samples to make the model more in line with actual market characteristics; At the same time, calibrate γ combined with expert judgment to ensure the controllability of constraints in extreme events and avoid model deviations caused by over-reliance on data.
(4) Balance global and regional operations: In the case, the differentiated distribution from the Shenzhen factory to retailers in Guangdong and warehouses in Malaysia (30,000 units and 90,000 units respectively) indicates that production and transportation plans need to be adjusted according to regional demand scales. Managers should establish a flexible production system, combine horizontal cooperation of local warehouses, take into account the personalized needs of regional markets in the global layout, and improve the overall efficiency of the supply chain through reasonable capacity allocation and inventory sharing.

7.2. Strategy analysis

Horizontal cooperation among multinational corporation at the same level is of great significance in the GSC. In the model proposed in this study, horizontal cooperation is primarily manifested through the sharing of historical data regarding customer locations and demands among warehouses. Subsequently, the distribution routes are coordinated and the resource allocation is optimized. We control the value of variable Y_j. When Y_j takes a binary value, it indicates the adoption of a horizontal cooperation strategy; when $Y_j = 1$, it indicates that all warehouses are being opened. Finally, we established multiple sets of experiments by modifying the total order quantity, where the order quantity is $R_1 = 990000, R_2 = 1380000, R_3 = 1690000, R_4 = 1990000, R_5 = 2380000$.

As shown in Fig. 6, taking Apple's sales supply chain in Guangdong, China and Malaysia as an example. When the horizontal cooperation strategy is not implemented, all warehouses function independently,

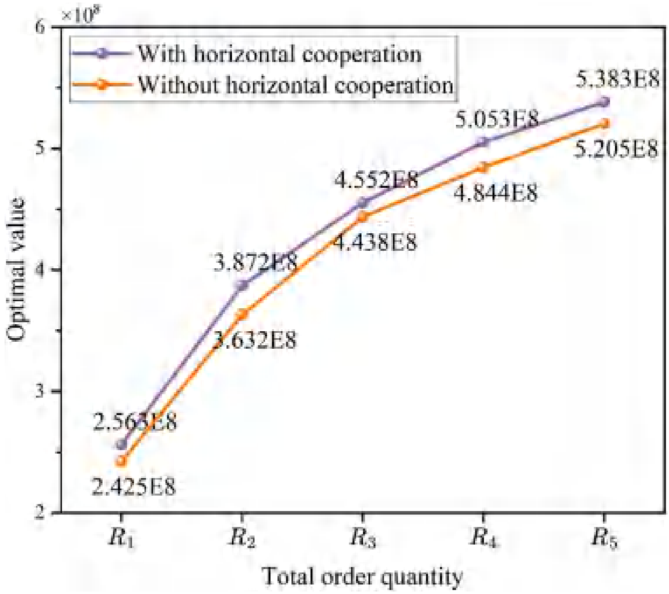

Fig. 7. The optimal value with and without horizontal cooperation.

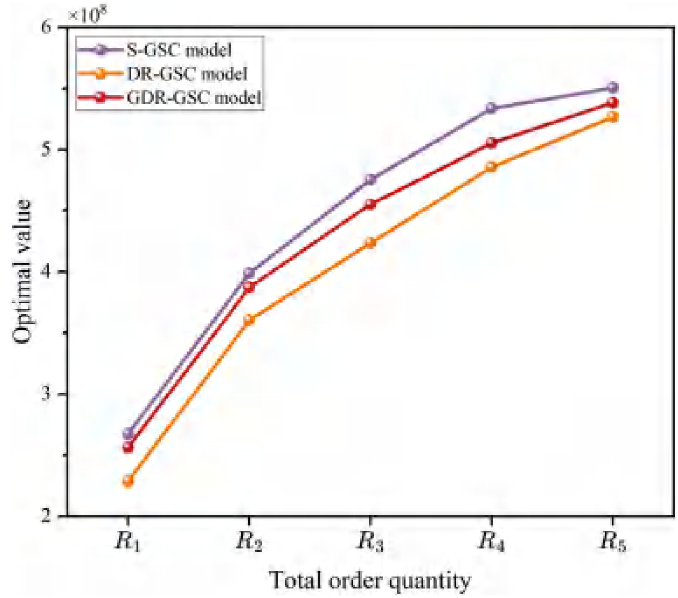

Fig. 8. Comparison of different models.

taking on the task of distribution in particular areas. After enabling horizontal cooperation, warehouse "W3" is no longer operational, and its originally responsible customers are assigned to warehouses "W2" and "W4". Consequently, the distribution routes and customer assignments have all changed. This change has brought significant advantages. Through the optimization of distribution routes, not only has the logistics cost been cut down, but also the service level has been elevated. Moreover, the overall operational efficiency of the supply chain has been significantly boosted. Meanwhile, resources have been allocated more rationally, thereby enhancing the flexibility of the supply chain.

Horizontal cooperation enables enterprises to better cope with the complex and changing market environment. In Fig. 7, the horizontal cooperation strategy has brought obvious profit growth. Multiple sets of experiments show that the profit of the experimental group adopting the horizontal cooperation strategy is higher than that of the control group without adopting it. Moreover, the profit growth in R_2 is as high as 6.25%. This fully proves the important value of horizontal cooperation in supply chain management and is an effective way for enterprises to achieve efficient and stable development.

7.3. Models comparison

In the prementioned section, we present a GDR model for GSC optimization under demand ambiguity. This subsection aims to provide a comparative analysis of the GDR-GSC model with the stochastic GSC model (S-GSC) and the distributionally robust GSC model (DR-GSC) to highlight the features and applications of the proposed GDR-GSC model.

We compare the different models using Apple's product sales data from the real-world example. In S-GSC model, we assume that the customers demand follows an uniform distribution, i.e., $\tilde{\boldsymbol{d}} \sim U(\hat{\boldsymbol{d}} - \Delta\boldsymbol{d}, \hat{\boldsymbol{d}} + \Delta\boldsymbol{d})$, the specific distribution is shown in Table 10. The DR-GSC model can be viewed as a special case of the GDR-GSC model. We adopt the outer ambiguity set in the GDR model as the ambiguity set of the DR model to capture the uncertainty of customer demand for calculating the optimal profit. Specifically, when we set $\gamma = 0$, the GDR-GSC model degenerates into the DR-GSC model. Finally, the results of three different models are plotted in Fig. 8.

When it comes to supply chain optimization models, a comprehensive analysis reveals significant insights. When comparing the three models in question, it is observed that the S-GSC model exhibits the highest optimal value among the three. Here we take the uniform distribution for the sake of calculation. However, it is important to note that the true distribution of customer demands in realistic is difficult to estimate. Nevertheless, ignoring the inaccuracy in the distribution may lead to serious decision-making risks.

Conversely, the DR-GSC model demonstrates the higher level of resilience when confronted with uncertain risk of random distribution. Nevertheless, this enhanced resilience comes at the expense of a relatively lower optimal value. This characteristic is at odds with the overarching objective of commercial companies, which is to maximize profits. In a business context, while risk mitigation is crucial, it must be balanced with the pursuit of profitability to ensure the viability of the enterprise.

Our proposed GDR-GSC model, on the other hand, strikes a balance between risk resistance and profit maximization. It is designed not only to provide a certain degree of protection against the risks of ambiguous distribution but also to maximize profits in supply chain as effectively as possible. Compared to DR-GSC model, the GDR-GSC model is well-suited for real-world supply chain scenarios, where managing the uncertainty and feasibility of constraints under a controllable violation level is of paramount importance. The GDR-GSC model offers a practical and effective solution for supply chain management in complex and uncertain environments.

8. Conclusion

The research presented in this paper contributes to the field of supply chain management by introducing a GDR-GSC model that addresses the challenges of demand ambiguity and horizontal cooperation. The GDR-GSC model is designed to optimize location and routing decisions within a GSC network, incorporating the complexities of production, transportation, and delivery process. The model's integration of the GDRO approach allows for a robust solution that considers worst-case scenarios and partial distributional information of demand ambiguity. This approach is particularly relevant in the current global business environment, where market dynamics and unforeseen events can significantly impact customer demand. The introduction of strengthened k-path cuts and tailored branching strategies further enhances the algorithm's performance, providing compact bounds and optimized

Table 10
Demand distribution of customer.

Customer	Demand	Customer	Demand
Kangar	$\tilde{d}_1 \sim U(10,000,20,000)$	Alor Setar	$\tilde{d}_2 \sim U(15,000,21,000)$
George Town	$\tilde{d}_3 \sim U(12,000,20,000)$	Kuala Terengganu	$\tilde{d}_4 \sim U(12,000,18,000)$
Shah Alam	$\tilde{d}_5 \sim U(10,000,18,000)$	Kuala Lumpur	$\tilde{d}_6 \sim U(12,000,20,000)$
Seremban	$\tilde{d}_7 \sim U(10,000,20,000)$	Kota Melaka	$\tilde{d}_8 \sim U(14,000,18,000)$
Johor Baharu	$\tilde{d}_9 \sim U(10,000,20,000)$	Putrajaya	$\tilde{d}_{10} \sim U(10,000,20,000)$
Ipoh	$\tilde{d}_{11} \sim U(10,000,20,000)$	Kuantan	$\tilde{d}_{12} \sim U(12,000,20,000)$
Kota Baharu	$\tilde{d}_{13} \sim U(14,000,18,000)$		

solutions. Our numerical experiments demonstrate the effectiveness and superiority of the customized B&C algorithm in solving the GDR-GSC model. The algorithm's ability to handle complex mixed-integer nonlinear programming problems is evident in its improved solution time and preserved solution quality. The case study based on Apple's sales in China and Malaysia illustrates the practical applicability of the GDR-GSC model. It showcases how the model can be used to analyze the impact of key parameters such as the radius of ambiguity set parameter θ and the global sensitivity parameter γ, offering valuable insights for strategic decision-making under ambiguity. The adoption of horizontal cooperation strategy in the GDR-GSC model is another significant contribution. By enabling warehouses to collaborate, the model demonstrates the potential for cost reduction, service level improvement, risk mitigation, enhanced flexibility, and sustainability. Finally, based on the comparison of our models, we prove that the GDR-GSC model has better performance, which can better resist risks and achieve relatively high optimal profit value.

Future research could focus on the considerations on other important factors in the supply chain, such as supply disruptions, environmental sustainability, and multiple products (Ren et al., 2024). This maybe incorporate additional constraints and variables into the GDR-GSC model to more accurately represent real-world supply chain scenarios. Additionally, further improvements in the exploration of more efficient solution methods could be investigated (Praxedes et al., 2024). This could involve exploring different branching strategies and cut generation techniques to further reduce the solution time and improve the solution quality. At the same time, we can consider multiple evaluation objectives related to the GSC. In addition to maximizing profit, other objectives such as minimizing lead times, or improving customer service levels could be incorporated (Hasani et al., 2021). This would push the use of the appropriate multi-objective optimization techniques and the analysis of trade-offs between different objectives.

CRediT authorship contribution statement

Zheng Wang: Writing – original draft, Methodology, Conceptualization. **Pingyuan Dong:** Software, Data curation, Conceptualization. **Ying Liu:** Writing – review & editing, Supervision, Formal analysis.

Declaration of competing interest

The authors declare that they have no known competing financial interests or personal relationships that could have appeared to influence the work reported in this paper.

Acknowledgments

The authors are extremely grateful to Editor-in-Chief and anonymous reviewers for their valuable comments, which helped us to improve the manuscript a lot. This work was supported by the Natural Science Foundation of Hebei Province, China [grant number A2023201020], the Operations Research and Management Innovation Team of Hebei University [grant number IT2023C02], the National Natural Science Foundation of China [grant number 61773150].

Appendix. Proof of Theorem 1

Proof. First, we prove the equivalent form of (15a). The GDR counterpart (15a) can be re-expressed as

$$\sup_{\mathbb{P}\in\mathcal{P}(\Xi),\mathbb{Q}\in\mathcal{F}_W(\theta)} \left\{ \mathbb{E}_{\mathbb{P}}\left[\sum_{k\in\mathcal{K}}\sum_{j\in\mathcal{L}} \tilde{d}_k f_{jkv} - Q\right] - \gamma_i d_W(\mathbb{P},\mathbb{Q}) \right\} \leq 0. \tag{29}$$

To establish strong duality through Lemma 1 of Liu et al. (2023), our model satisfies all necessary conditions: (i) the feasible set Ξ, as a constructed bounded polyhedron, is compact; (ii) $\mathbb{E}_{\mathbb{P}}\left[\sum_{k\in\mathcal{K}}\sum_{j\in\mathcal{L}} \tilde{d}_k f_{jkv} - Q\right]$ is proper, closed, and convex in $d_W(\cdot,\cdot)$; (iii) the Wasserstein ambiguity set $\mathcal{F}_W(\theta)$ maintains a non-empty interior through the moment constraint $d_W\left(\mathbb{P},\hat{\mathbb{P}}\right) \leq \theta$; and (iv) $\sum_{k\in\mathcal{K}}\sum_{j\in\mathcal{L}} \tilde{d}_k f_{jkv} - Q$ is Lipschitz continuity on Ξ, since it is an affine function. Thus, the regularity conditions of Lemma 1 are satisfied, and we can obtain

$$\begin{aligned}&\sup_{\mathbb{P}\in\mathcal{P}(\Xi),\mathbb{Q}\in\mathcal{F}_W(\theta)} \left\{ \mathbb{E}_{\mathbb{P}}\left[\sum_{k\in\mathcal{K}}\sum_{j\in\mathcal{L}} \tilde{d}_k f_{jkv} - Q\right] - \gamma_1 d_W(\mathbb{P},\mathbb{Q}) \right\}\\ &= \inf_{t^1\in[0,\gamma_1]} \left\{ \theta t^1 + \frac{1}{N}\sum_{n\in\mathcal{N}} \sup_{\boldsymbol{d}\in\Xi} \left\{ \sum_{k\in\mathcal{K}}\sum_{j\in\mathcal{L}} \hat{d}_{kn} f_{jkv} - Q - t^1 \left\|\tilde{\boldsymbol{d}} - \hat{\boldsymbol{d}}_n\right\| \right\} \right\}.\end{aligned} \tag{30}$$

Given s_n^1, $\boldsymbol{\mu}_n^1$ and $\boldsymbol{\varpi}_n^1 \in \mathbb{R}^K$ are introduced arbitrary variables, we can convert the right-hand side of (30) into the following constraints:

$$\begin{cases} \theta N t^1 + \sum_{n\in\mathcal{N}} s_n^1 \leq 0, \\ \sup_{\boldsymbol{d}\in\Xi} \left\{ \sum_{k\in\mathcal{K}}\sum_{j\in\mathcal{L}} \hat{d}_{kn} f_{jkv} - Q - t^1 \left\|\tilde{\boldsymbol{d}} - \hat{\boldsymbol{d}}_n\right\| \right\} \leq s_n^1, \\ t^1 \in [0,\gamma_1]. \end{cases} \tag{31}$$

Introducing arbitrary variables $\boldsymbol{\mu}_n^1$ and $\boldsymbol{\varpi}_n^1 \in \mathbb{R}^K$, based on Theorem 2 in Mohajerin Esfahani and Kuhn (2018), we transform (31) into the equivalent form:

$$\begin{cases} \theta N t^1 + \sum_{n\in\mathcal{N}} s_n^1 \leq 0, \\ \left[-\left(\sum_{k\in\mathcal{K}}\sum_{j\in\mathcal{L}} \hat{d}_{kn} f_{jkv} - Q\right)\right]^* (\boldsymbol{\mu}_n^1 - \boldsymbol{\varpi}_n^1) \\ +\delta^*(\boldsymbol{\varpi}_n^1|\Xi) - \hat{\boldsymbol{d}}_n^T \boldsymbol{\mu}_n^i \leq s_n^1, \forall v\in\mathcal{V}, \forall n\in\mathcal{N}, \\ \left\|\boldsymbol{\mu}_n^1\right\|_* \leq t^1, \forall n\in\mathcal{N}, \\ t^1 \in [0,\gamma_1]. \end{cases} \tag{32}$$

Let $g(\hat{\boldsymbol{d}}_n) = \sum_{k\in\mathcal{K}}\sum_{j\in\mathcal{L}} \hat{d}_{kn} f_{jkv} - Q$. Since the function g is in the form of an affine sum, its conjugate function takes the following form:

$$g^*(\hat{\boldsymbol{d}}_n) = \begin{cases} Q, & \boldsymbol{\mu}_n^1 = \boldsymbol{\varpi}_n^1, \\ \infty, & \boldsymbol{\mu}_n^1 \neq \boldsymbol{\varpi}_n^1. \end{cases} \tag{33}$$

By setting $\psi_n^1 = [\boldsymbol{\omega}_n^1; \tau_n^1]$, the conjugate of the support function $\delta^*(\boldsymbol{\varpi}_n^1|\Xi)$ can be expressed as:

$$\begin{aligned}\delta^*(\boldsymbol{\varpi}_n^1|\Xi) &= \sup_{\boldsymbol{\varpi}_n^1}\{\boldsymbol{\varpi}_n^1\hat{\boldsymbol{d}}_n \,:\, A\hat{\boldsymbol{d}}_n + \boldsymbol{c} \in K\} \\ &= \inf_{\psi_n^1}\{\boldsymbol{c}^T\psi_n \,:\, {\psi_n^1}^T\hat{\boldsymbol{d}}_n = -\boldsymbol{\varpi}_n^1, \boldsymbol{\varpi}_n^1 \in K_*\},\end{aligned} \tag{34}$$

where $K = \{(\tau_n^1, \boldsymbol{\omega}_n^1) \in \mathbb{R}\times\mathbb{R}^K \,:\, \tau_n^1 \geq \|\boldsymbol{\omega}_n^1\|_\infty\}$, the dual cone is $K_* = \{(\tau_n^1, \boldsymbol{\omega}_n^1) \in \mathbb{R}\times\mathbb{R}^K \,:\, \tau_n^1 \geq \|\boldsymbol{\omega}_n^1\|_1\}$. Then, by substituting Eqs. (33) and (34) into formula (32), formula (32) can be transformed into the following form:

$$\begin{cases} \theta N t^1 + \sum_{n\in\mathcal{N}} s_n^1 \leq 0, \\ -Q + \hat{\boldsymbol{d}}_n^T \sum_{j\in\mathcal{K}} \boldsymbol{f}_{jv} + \omega_n^1\hat{\boldsymbol{d}}_n + \Lambda\tau_n^1 \leq s_n^1, \forall n\in\mathcal{N}, \forall v\in\mathcal{V}, \\ \left\|\boldsymbol{\omega}_n^1 + \sum_{j\in\mathcal{L}} \boldsymbol{f}_{jv}\right\|_\infty \leq t^1, \forall v\in\mathcal{V}, \forall n\in\mathcal{N}, \\ \tau_n^1 \geq \left\|\boldsymbol{\omega}_n^1\right\|_1, \forall n\in\mathcal{N}, \\ t^1 \in [0, \gamma_1]. \end{cases}$$

Similarly, the tractable counterparts of constraints (15b) and (15c) can be obtained.

The proof of theorem is complete. □

Data availability

Data will be made available on request.

References

Bakhshi Sasi, M., Sarker, R.A., Essam, D.L., 2024. A novel heuristic algorithm for disruption mitigation in a global food supply chain. Comput. Ind. Eng. 194, 110334. http://dx.doi.org/10.1016/j.cie.2024.110334.

Beale, E.M.L., Forrest, J.J.H., 1976. Global optimization using special ordered sets. Math. Program. 10, 52–69. http://dx.doi.org/10.1007/BF01580653.

Ben-Tal, Brekelmans, R., Den Hertog, D., Vial, J.-P., 2017. Globalized robust optimization for nonlinear uncertain inequalities. INFORMS J. Comput. 29, 350–366. http://dx.doi.org/10.1287/ijoc.2016.0735.

Ben-Tal, A., Ghaoui, L.E., Nemirovski, A., 2009. Robust Optimization, first ed. Princeton University Press, Oxfordshire.

Birge, J.R., Louveaux, F., 2011. Introduction To Stochastic Programming, second ed. Springer Science & Business Media, New York.

Chen, Z., Hammad, A.W.A., Alyami, M., 2024. Building construction supply chain resilience under supply and demand uncertainties. Autom. Constr. 158, 105190. http://dx.doi.org/10.1016/j.autcon.2023.105190.

Costa, L., Contardo, C., Desaulniers, G., 2019. Exact branch-price-and-cut algorithms for vehicle routing. Transp. Sci 53 (4), 946–985. http://dx.doi.org/10.1287/trsc.2018.0878.

De Farias, I.R., Zhao, M., Zhao, H., 2008. A special ordered set approach for optimizing a discontinuous separable piecewise linear function. Oper. Res. Lett. 36 (2), 234–238. http://dx.doi.org/10.1016/j.orl.2007.05.004.

Dey, S.S., Dubey, Y., Molinaro, M., Shah, P., 2024. A theoretical and computational analysis of full strong-branching. Math. Program. 205 (1–2), 303–336. http://dx.doi.org/10.1007/s10107-023-01977-x.

Dong, Q., Yuan, Y., 2025. Data-driven distributionally robust supplier selection and order allocation problems considering carbon emissions. Int. Tran. Oper. Res 32 (2), 1119–1145. http://dx.doi.org/10.1111/itor.13328.

Duan, H.W., Zhang, L.P., Gan, B., Chang, X., Wang, X.F., Li, K.H., 2023. A system dynamicsbased simulation model for cross-border logistics risk transmission. Int. J. Simul. Model. 22 (3), 485–496. http://dx.doi.org/10.2507/IJSIMM22-3-CO11.

Elyasi, M., Altan, B., Ekici, A., Özener, O.Ö., Yanıkoğlu, İ., Dolgui, A., 2024. Production planning with flexible manufacturing systems under demand uncertainty. Int. J. Prod. Res. 62 (1–2), 157–170. http://dx.doi.org/10.1080/00207543.2023.2288722.

Enayati, S., Özaltın, O.Y., 2024. Supplier selection under disruption risk with hybrid procurement. Comput. Oper. Res. 165, 106593. http://dx.doi.org/10.1016/j.cor.2024.106593.

Fan, X., Yin, Z., Liu, Y., 2020. The value of horizontal cooperation in online retail channels. Electron. Commer. R. A 39, 100897. http://dx.doi.org/10.1016/j.elerap.2019.100897.

Gao, S., Liu, Yankui, Liu, Ying, 2024. Designing robust green sustainable supply chain network by bi-objective optimization method. Int. J. Gen. Syst. 53 (4), 453–484. http://dx.doi.org/10.1080/03081079.2023.2292663.

Hacardiaux, T., Tancrez, J.-S., 2020. Assessing the environmental benefits of horizontal cooperation using a location-inventory model. Central Eur. J. Oper. Res 28, 1363–1387. http://dx.doi.org/10.1007/s10100-018-0599-7.

Hacardiaux, T., Tancrez, J.-S., 2022. Assessing the benefits of horizontal cooperation for the various stages of the supply chain. Oper. Res. 22 (4), 3901–3924. http://dx.doi.org/10.1007/s12351-021-00688-5.

Hasani, A., Mokhtari, H., Fattahi, M., 2021. A multi-objective optimization approach for green and resilient supply chain network design: a real-life case study. J. Clean. Prod 278, 123199. http://dx.doi.org/10.1016/j.jclepro.2020.123199.

Hosseinnezhad, D., Nugroho, Y.K., Heavey, C., 2023. Horizontal collaboration between suppliers to mitigate supply chain disruption: a secure resource sharing strategy. Comput. Ind. Eng. 177, 109088. http://dx.doi.org/10.1016/j.cie.2023.109088.

Khan, E.A., 2020. Logistics & Supply Chain Management (Doctoral dissertation). College of Management and Economics Studies, UPES, Dehradun, https://dr.ddn.upes.ac.in/handle/123456789/3838.

Kim, J., Chung, B.D., Kang, Y., Jeong, B., 2018. Robust optimization model for closed-loop supply chain planning under reverse logistics flow and demand uncertainty. J. Clean. Prod 196, 1314–1328. http://dx.doi.org/10.1016/j.jclepro.2018.06.157.

Kou, S., Golden, B., Bertazzi, L., 2024. An improved model for estimating optimal VRP solution values. Optim. Lett. 18, 697–703. http://dx.doi.org/10.1007/s11590-023-02082-w.

Koyuncuoğlu, M.U., Demir, L., 2023. An adaptive hybrid variable-large neighborhood search algorithm for profit maximization problem in designing production lines. Comput. Ind. Eng. 175, 108871. http://dx.doi.org/10.1016/j.cie.2022.108871.

Lalmazloumian, M., Wong, K.Y., Govindan, K., Kannan, D., 2016. A robust optimization model for agile and build-to-order supply chain planning under uncertainties. Ann. Oper. Res. 240 (2), 435–470. http://dx.doi.org/10.1007/s10479-013-1421-5.

Li, R., Cui, Z., Kuo, Y.-H., Zhang, L., 2023. Scenario-based distributionally robust optimization for the stochastic inventory routing problem. Transp. Res. Part E Logist. Transp. Rev 176, 103193. http://dx.doi.org/10.1016/j.tre.2023.103193.

Li, H., Li, R., Shang, M., Liu, Y., Su, D., 2022. Cooperative decisions of competitive supply chains considering carbon trading mechanism. Int. J. Low-Carbon Technol 17, 102–117. http://dx.doi.org/10.1093/ijlct/ctab085.

Li, J., Xiong, N., Park, J.H., Liu, C., Ma, S., Cho, S., 2012. Intelligent model design of cluster supply chain with horizontal cooperation. J. Intell. Manuf. 23 (4), 917–931. http://dx.doi.org/10.1007/s10845-009-0359-6.

Lin, F., Fang, X., Gao, Z., 2022. Distributionally robust optimization: a review on theory and applications. Numer. Algebra, Control. Optim 12 (1), 159–212. http://dx.doi.org/10.3934/naco.2021057.

Liu, F., Chen, Z., Wang, S., 2023. Globalized distributionally robust counterpart. INFORMS J. Comput. 35 (5), 1120–1142. http://dx.doi.org/10.1287/ijoc.2022.0274.

Lotfi, M., Larmour, A., 2021. Supply chain resilience in the face of uncertainty: how horizontal and vertical collaboration can help? Cont. Resil. Rev 4, 37–53. http://dx.doi.org/10.1108/CRR-04-2021-0016.

Luo, F., Mehrotra, S., 2019. Decomposition algorithm for distributionally robust optimization using wasserstein metric with an application to a class of regression models. European J. Oper. Res. 278 (1), 20–35. http://dx.doi.org/10.1016/j.ejor.2019.03.008.

Mohajerin Esfahani, P., Kuhn, D., 2018. Data-driven distributionally robust optimization using the wasserstein metric: performance guarantees and tractable reformulations. Math. Program. 171, 115–166. http://dx.doi.org/10.1007/s10107-017-1172-1.

Nguyen, D.H., Chen, H., 2018. Supplier selection and operation planning in biomass supply chains with supply uncertainty. Comput. Chem. Eng. 118, 103–117. http://dx.doi.org/10.1016/j.compchemeng.2018.07.012.

Niu, B., Wang, L., Dong, J., 2023. Enabling emergency production shifting: the value of blockchain in supply chain resilience confronting COVID-19. Risk Anal. 1–31. http://dx.doi.org/10.1111/risa.14199.

Ortega, F., Wolsey, L.A., 2003. A branch-and-cut algorithm for the single-commodity, uncapacitated, fixed-charge network flow problem. Networks 41 (3), 143–158. http://dx.doi.org/10.1002/net.10068.

Peivastehgar, H.R., Divsalar, A., Paydar, M.M., Chitsaz, M., 2023. A green production routing problem for medical nitrous oxide: model and solution approach. Expert Syst. Appl. 230, 120704. http://dx.doi.org/10.1016/j.eswa.2023.120704.

Petridis, K., Dey, P.K., Chattopadhyay, A.K., Boufounou, P., Toudas, K., Malesios, C., 2023. A stochastically optimized two-echelon supply chain model: an entropy approach for operational risk assessment. Entropy-Switz 25 (9), 1245. http://dx.doi.org/10.3390/e25091245.

Praxedes, R., Bulhões, T., Subramanian, A., Uchoa, E., 2024. A unified exact approach for a broad class of vehicle routing problems with simultaneous pickup and delivery. Comput. Oper. Res. 162, 106467. http://dx.doi.org/10.1016/j.cor.2023.106467.

Qu, S., Meng, D., Zhou, Y., Dai, Y., 2017. Distributionally robust games with an application to supply chain. J. Intell. Fuzzy Syst 33 (5), 2749–2762. http://dx.doi.org/10.3233/JIFS-169324.

Quintero-Araujo, C.L., Gruler, A., Juan, A.A., Faulin, J., 2019. Using horizontal cooperation concepts in integrated routing and facility-location decisions. Int. Tran. Oper. Res 26, 551–576. http://dx.doi.org/10.1111/itor.12479.

Ren, H., Mu, D., Wang, C., Yue, X., Li, Z., Du, J., Zhao, L., Lim, M.K., 2024. Vulnerability to geopolitical disruptions of the global electric vehicle lithium-ion battery supply chain network. Comput. Ind. Eng. 188, 109919. http://dx.doi.org/10.1016/j.cie.2024.109919.

Saeed, N., 2013. Cooperation among freight forwarders: mode choice and intermodal freight transport. Res. Transp. Econ 42 (1), 77–86. http://dx.doi.org/10.1016/j.retrec.2012.11.005.

Saif, A., Madani, N., 2022. Robust design of service systems with immobile servers under demand uncertainty. Comput. Oper. Res. 148, 105965. http://dx.doi.org/10.1016/j.cor.2022.105965.

Sarkar, B., Debnath, A., Chiu, A.S.F., Ahmed, W., 2022. Circular economy-driven two-stage supply chain management for nullifying waste. J. Clean. Prod 339, 130513. http://dx.doi.org/10.1016/j.jclepro.2022.130513.

Seman, L.O., Rigo, C.A., Camponogara, E., Bezerra, E.A., Coelho, L. dos S., 2023. Explainable column-generation-based genetic algorithm for knapsack-like energy aware nanosatellite task scheduling. Appl. Soft Comput. 144, 110475. http://dx.doi.org/10.1016/j.asoc.2023.110475.

Shi, R., Zhang, J., Ru, J., 2013. Impacts of power structure on supply chains with uncertain demand. Prod. Oper. Manag. 22 (5), 1232–1249. http://dx.doi.org/10.1111/poms.12002.

Sirikasemsuk, K., Luong, H.T., 2017. Measure of bullwhip effect in supply chains with first-order bivariate vector autoregression time-series demand model. Comput. Oper. Res. 78, 59–79. http://dx.doi.org/10.1016/j.cor.2016.08.005.

Soysal, M., Bloemhof-Ruwaard, J.M., Haijema, R., van der Vorst, J.G.A.J., 2018. Modeling a green inventory routing problem for perishable products with horizontal collaboration. Comput. Oper. Res. 89, 168–182. http://dx.doi.org/10.1016/j.cor.2016.02.003.

Tan, Y., Zhao, W., Guo, C., 2021. The joint procurement model and algorithm for small and medium enterprises. Comput. Ind. Eng. 155, 107179. http://dx.doi.org/10.1016/j.cie.2021.107179.

Timmer, M.P., Los, B., Stehrer, R., de Vries, G.J., 2021. Supply chain fragmentation and the global trade elasticity: A new accounting framework. Imf. Econ. Rev. 69 (4), 656. http://dx.doi.org/10.1057/s41308-021-00134-8.

Tokito, S., Hanaka, T., Nagashima, F., 2023. Structural attribution of emissions along the global supply chain and implications for climate policy. J. Ind. Ecol 27 (6), 1488–1499. http://dx.doi.org/10.1111/jiec.13428.

Tsai, C.-F., Chao, K.-M., 2009. Chromosome refinement for optimising multiple supply chains. Inf. Sci 179 (14), 2403–2415. http://dx.doi.org/10.1016/j.ins.2009.03.009.

Wang, M., Amiri-Aref, M., Klibi, W., Babai, M.Z., 2024a. Global multi-sourcing network design with inventory planning under uncertainty. Int. J. Prod. Res. 62 (21), 7660–7686. http://dx.doi.org/10.1080/00207543.2024.2323068.

Wang, Y., Ma, H., Liu, Y., 2025. Sustainable food waste supply chain network design problem with government environmental oversight: globalized robust bi-level model and exact algorithm. Soc. Econ. Plann. Sci 99, 102205. http://dx.doi.org/10.1016/j.seps.2025.102205.

Wang, M., Ouyang, J., Zhao, L., 2021. Production planning with transshipment in a global supply chain under different carbon trading mechanisms. Oper. Res. 21, 2309–2331. http://dx.doi.org/10.1007/s12351-019-00518-9.

Wang, S., Yang, G., Liu, S., 2024b. A data-driven multi-channel supply chain multi-factory collaborative production planning problem. Soft Comput. http://dx.doi.org/10.1007/s00500-023-09546-2.

Wang, Q., Zhang, M., Li, R., 2024c. The COVID-19 pandemic and supply chain: international cooperation patterns and influence mechanism. Benchmarking: Int. J. 31 (2), 466–486. http://dx.doi.org/10.1108/BIJ-04-2022-0257.

Wei, J., Gao, S., Liu, Y., 2024. Modeling uncertain multi-objective production and outbound distribution scheduling problem with customised products. Int. J. Syst. Sci.: Oper. Logist 11 (1), 2407360. http://dx.doi.org/10.1080/23302674.2024.2407360.

Wen, M., Larsen, R., Ropke, S., Petersen, H.L., Madsen, O.B.G., 2019. Centralised horizontal cooperation and profit sharing in a shipping pool. J. Oper. Res. Soc..

World Economic Forum, 2022. The global risks report 2022. https://www3.weforum.org/docs/WEF_The_Global_Risks_Report_2022_CN.pdf. (Accessed 25 September 2024).

Wu, J., Shang, J., 2021. Green credit financing equilibrium under government subsidy and supply uncertainty. Sustainability 13 (22), 12917. http://dx.doi.org/10.3390/su132212917.

Yang, D., 2021. The trend and key influencing factors of global industrial chain reconstruction. Rmll. Xsqy 7, 32–40. http://dx.doi.org/10.16619/j.cnki.rmltxsqy.2022.07.005.

Yang, L., Zhang, Q., Ji, J., 2017. Pricing and carbon emission reduction decisions in supply chains with vertical and horizontal cooperation. Int. J. Prod. Econ. 191, 286–297. http://dx.doi.org/10.1016/j.ijpe.2017.06.021.

Yazdekhasti, A., Wang, J., Zhang, L., Ma, J., 2021. A multi-period multi-modal stochastic supply chain model under COVID pandemic: a poultry industry case study in mississippi. Transp. Res. Part E Logist. Transp. Rev 154, 102463. http://dx.doi.org/10.1016/j.tre.2021.102463.

You, F., Grossmann, I.E., 2013. Multicut benders decomposition algorithm for process supply chain planning under uncertainty. Ann. Oper. Res. 210 (1), 191–211. http://dx.doi.org/10.1007/s10479-011-0974-4.

Zhang, P., Liu, Y., Yang, G., Zhang, G., 2022. A distributionally robust optimisation model for last mile relief network under mixed transport. Int. J. Prod. Res. 60 (4), 1316–1340. http://dx.doi.org/10.1080/00207543.2020.1856439.

Zhao, B., Su, K., Wei, Y., Shang, T., 2024. Design of distributionally robust closed-loop supply chain network based on data-driven under disruption risks. Int. J. Syst. Sci.: Oper. Logist 11 (1), 2309293. http://dx.doi.org/10.1080/23302674.2024.2309293.

Zhen, L., Huang, L., Wang, W., 2019. Green and sustainable closed-loop supply chain network design under uncertainty. J. Clean. Prod 227, 1195–1209. http://dx.doi.org/10.1016/j.jclepro.2019.04.098.